Article

Provenance of Heavy Minerals: A Case Study from the WNW Portuguese Continental Margin

João Cascalho

Instituto D. Luiz and Departamento de Geologia, Faculdade de Ciências (Universidade de Lisboa), Edifício C6, Campo Grande, 1749-016 Lisboa, Portugal; jpcascalho@ciencias.ulisboa.pt

Abstract: This work describes and interprets the presence of heavy minerals in the WNW Portuguese continental margin using a set of 78 bottom samples collected from three distinct areas of this margin: the Porto, Aveiro, and Nazaré canyon head areas. The main transparent heavy mineral assemblage (mineral grains with frequencies ≥1% identified under a petrographic microscope) is composed of amphibole, andalusite, tourmaline, biotite, garnet, staurolite, pyroxene, zircon, and apatite. The felsic igneous and metamorphic rock outcrops in the main Northern Portuguese river basins and the relict sedimentary continental shelf deposits explained the presence of most of these mineral grains (both considered as distal sources). However, the presence of pargasite, augite, diopside-hedenbergite, enstatite-ferrosilite, and forsterite in the Porto and Aveiro areas (minerals identified by electronic microprobe analysis) is probably related to the presence of an igneous basic source next to dolomitic limestones affected by thermal metamorphism. These geological formations are considered as local sources. The high concentration of biotite observed in the Nazaré area is the result of the selective transport of the most lamellar sand particles of this mineral.

Keywords: mineral grains composition; surface textures; sources; WNW Portuguese Continental Margin

1. Introduction

> *"Thus, we live in a universe primed for complexification: hydrogen atoms form stars, stars form the elements of the periodic table, those elements form planets, which in turn form minerals abundantly. Minerals catalyze the formation of biomolecules, which on Earth led to life. In this sweeping scenario, minerals represent but one inexorable step in the evolution of a cosmos that is learning to know itself."*
> [1] (p.58)

The presence of heavy minerals in sedimentary deposits represents a detrital occurrence of either constituent or accessory rock-forming minerals. Consequently, they have been used as an important tool to understand sedimentary processes and to identify operating factors that control depositional environments [2]. For example, on continental margins and on littoral environments, heavy mineral analysis is often used to diagnose sediment sources, to trace sand transport paths, to understand grain sorting processes, to deduce energy levels of transporting agents, and to interpret global sediment provenance in terms of sedimentary cycles [3–6]. Normally the presence of these minerals is easier to interpret on terrestrial and coastal environments than on continental shelf areas. This is because the direct relationship between sourcing/distributor processes and sedimentary deposits is more straightforward in the accessible terrestrial and coastal environments than on the underwater continental shelf areas that usually contain a mixture of relict and modern sedimentary particles [7,8]. The presence of heavy minerals on the Northern Portuguese continental shelf and corresponding coastal areas is mentioned in several works published over the last decades, from where it is possible

to know their distribution patterns [9–11]. Biotite, andalusite, zircon, tourmaline, apatite, amphibole, garnet, and staurolite are referred on those works as the main transparent mineral species. A first attempt to interpret the provenance of these minerals pointed to rocky outcrops from the watersheds of the Northern Portuguese rivers as the most probable sources. Hence, the main sources for these minerals were attributed to metamorphic and felsic igneous rocks of the Old Iberian Massif [12]. However, the presence of a mafic mineral assemblage composed by "brown hornblende", pyroxene, and olivine initially detected south of Porto canyon in the early 1990s, it was explained at that time by the existence of a nearby source made up of some kind of basic igneous rocks [9]. Later, based on the acquisition of the first mineral chemical composition data (microprobe analysis) it was discovered that this mafic assemblage was composed by pyroxenes of diopside-hedenbergite, enstatite-ferrosilite, and augite compositions, and by olivine with dominant forsterite composition [10]. It should be noted that this mineralogical assemblage was only found on the south of Porto's canyon and at depths exceeding 100 m, which led [12] to state the probable existence of an igneous basic source located "in the outer shelf/upper slope south of Porto canyon" [12] (p. 99). It turns out that the presence of these minerals was described through chemical composition analysis, expressed by the percentage of oxides that were present. Therefore, the relationship between these minerals and their specific sources has never been properly interpreted using suitable mineralogical diagrams. In addition to these findings, seismic data and remote operated vehicle (ROV) images of the seafloor near the Porto upper canyon head area obtained by [13] showed the existence of a geological structure of possible volcanic origin. This structure was described as a rock relief at more than 15 m in height, standing out from neighboring geological formations being recognized in a seismic profile by a very distinctive diffractive hyperbola [13]. Its presence was attributed to a hard rock body (of dolomitic nature) that stands out from the nesting sedimentary rocks (detrital sediments with evidence of carbonate cement). The heavy mineral assemblage of the Nazaré canyon area stands out from the assemblages of Porto and Aveiro areas because of the absence of pyroxene and olivine and by the high frequency of biotite mineral grains [11]. Due to its localization, Nazaré's canyon head remains active in capturing sedimentary particles transported by littoral drift and along the inner continental shelf [14–16]. Despite the existence of all this relevant information, it happens that in the surrounding areas of the Porto, Aveiro and Nazaré canyons heads (Figure 1), the relationship of the referred mineral species with specific sources has never been properly investigated. Thus, to study this relationship in detail, the present work uses 78 sea bottom samples collected from Porto, Aveiro, and Nazaré canyon upper head areas, from which the identification of transparent heavy minerals was made. This identification is based on two different datasets. One of them concerns the optical identification of the transparent heavy minerals. The other set uses the chemical composition of heavy mineral grains obtained by microprobe analysis. This second dataset includes old mineral chemical composition results covering the Northern Portuguese continental shelf [10], and new mineral chemical composition results from four samples collected from the Porto canyon head area. Thus, the central issue that is addressed in this work is the search of the specific sources for the main transparent heavy minerals identified in the three target areas, Porto, Aveiro, and Nazaré canyon head areas, considering the supply and distribution of sedimentary particles in the Western Portuguese continental margin.
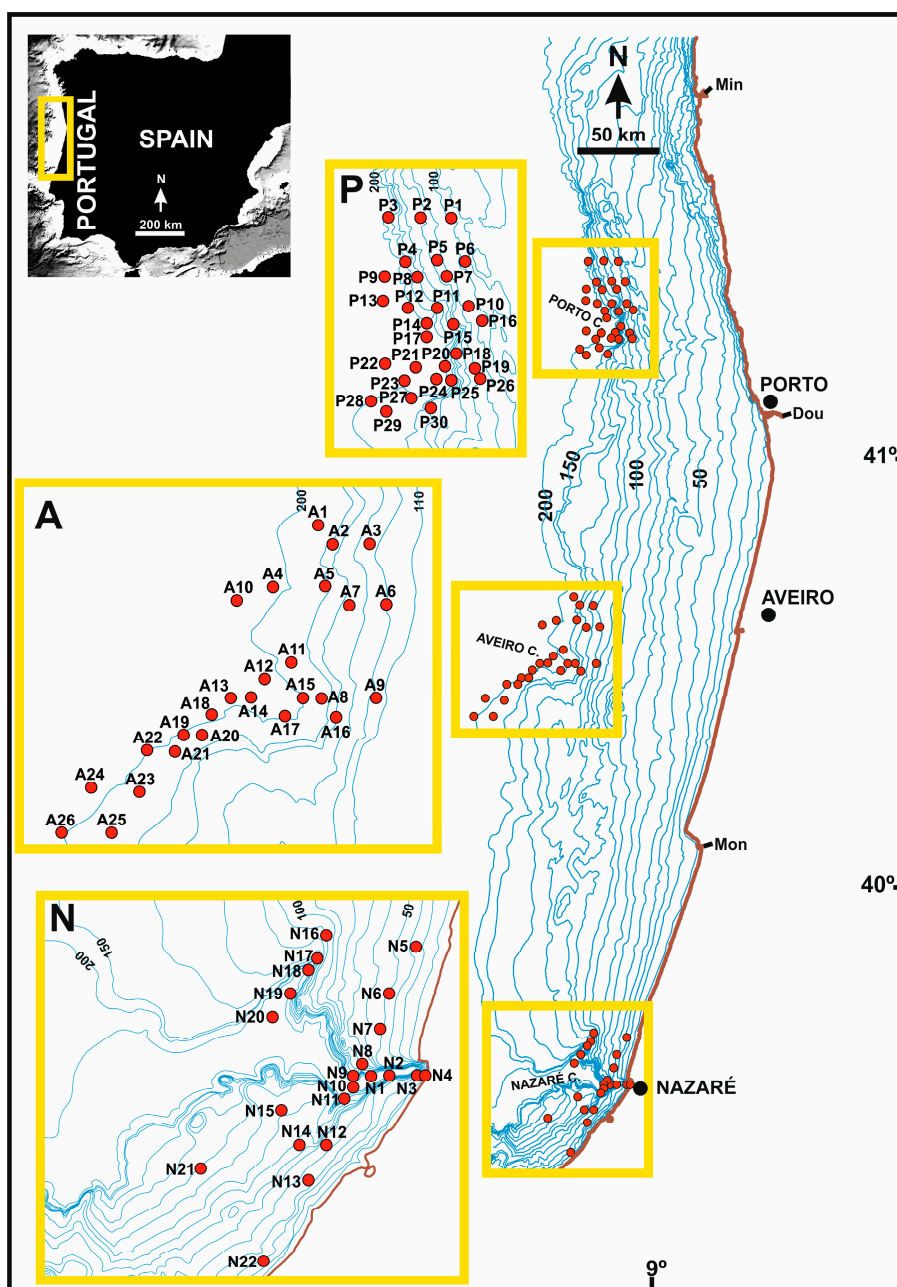
Figure 1. Location of the samples according the three studies areas: Porto (P), Aveiro (A), and Nazaré (N) canyon head areas. Min, Minho River; Dou, Douro River; Mon, Mondego River. Bathymetric contour lines are in meters.

2. Geological Setting

Porto, Aveiro, and Nazaré canyons are important geomorphologic features of the WNW Portuguese continental margin. However, while the Porto and Aveiro canyons are considered as minor submarine valleys because they weakly indent the shelf [17], the Nazaré canyon is one of the largest canyons of the European Margin (170 km) and it cuts the entire width of the Portuguese Margin, from the Iberia Abyssal Plain (at a 5000 m depth) to the infralittoral zone off the Nazaré beach [18]. The geological nature of the canyon heads surrounding the area is also different: The Porto canyon is carved in carbonated to detrital rocks that are highly dolomitized, of Paleocene age; the Aveiro canyon is carved in biogenic and detrital limestones rocks of Neogenic and Eocenic ages; and the Nazaré canyon is carved on Mesozoic rocks (essentially limestones) [13,18].

The sedimentary cover of the referred canyon head's surrounding areas is mainly composed of sand with the presence of some other deposits enriched in gravel or silt particles [19]. The Porto area reveals a higher grain size variability, ranging between sand and gravel at shallower depths (less than 100 m) up to fine sediment particles (silt and clay), which is well represented at the middle shelf (Douro muddy deposit) and upper slope where some isolated spots of these finer particles reach up to 70% of the sediment total weight [19]. The Aveiro area reveals a more homogenous sedimentary cover where sand is the dominant textural type, always representing more than 60% of the total sediment. In some small areas between 100 and 150 m in depth, the gravel particles represent up to $^1/_3$ of the total sediment. Finer sediments are only important in some small areas of the upper continental slope with almost 30% of the total sediment weight [19]. The shelf sedimentary cover near the Nazaré canyon is dominated by coarse-grained particles (sandy gravel) in some locations, namely at 40–80 m in depth. At these depths, these particles constitute a sedimentary deposit with a geometry sub-parallel to the coast line orientation (paleo littorals). Fine and very fine sands have been recorded in the inner shelf north of the canyon and close to its head. Additionally, two important muddy deposit areas are present in the middle shelf north and south of this canyon, at approximately 100 m in depth [14,20]. Most of the Norwest of Iberian Peninsula in an area corresponding to the main river basins is characterized by the presence of Precambrian and Paleozoic igneous (mainly granites) and metamorphic rocks (mainly schists, gneisses, and graywackes). These old rocks are covered by more recent terrains (of Mesozoic and Cenozoic ages) composed by detrital and carbonate sedimentary rocks correspondent to the Douro basin and to the Portuguese Occidental sedimentary basin (known as the Lusitanian basin) (Figure 2).
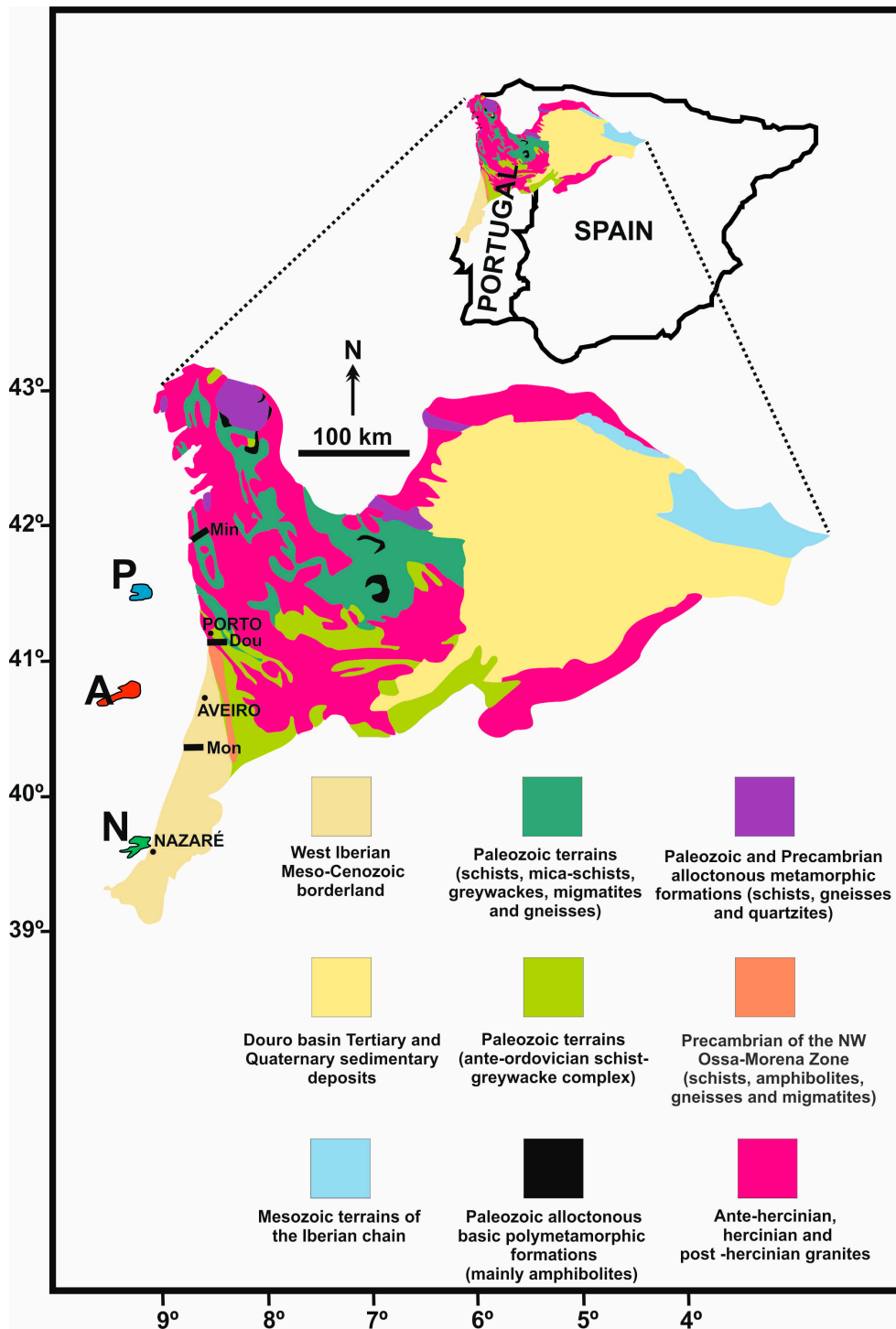
Figure 2. Simplified geological map considering the areas of the main northern Iberian Peninsula and Portuguese river basins: Minho (Min), Douro (Dou) and Mondego (Mon). P, A, and N represent the location of the sea bottom areas with samples collected respectively from Porto, Aveiro, and Nazaré upper canyon areas (adapted from [21]).

The referred igneous and metamorphic rocks can be considered as primary sources and the more recent terrains (of West Iberian Meso-Cenozoic borderland) can be considered as sedimentary sources of the heavy minerals found in the three studied areas. According to [22–32] these geological formations have a diverse heavy mineral composition that is summarized in Table 1.

Table 1. Heavy mineral composition of the main igneous and metamorphic rocks and from the sedimentary rocks from the West Iberian Meso-Cenozoic borderland. These geological formations are present in the Portuguese north and western river basins (based on the information contained in works [22–31].

Source Rocks	Location (River Basin)	Heavy Minerals
Granites	Outcropping in the six Portuguese northern river basins (from Minho to Mondego). Main outcrops are present in Minho, Lima, Ave and Cávado river basins.	Biotite, tourmaline, apatite, zircon, rutile, amphibole and iron, titanium oxides, and occasionally garnet.
Micaschists, gneisses and migmatites	Outcropping in the SW limit of Douro basin (Douro River mouth) and near the coastal zone south of the Douro river.	Biotite, garnet, sillimanite, apatite, and zircon.
Amphibolites and amphibolitic schists	Outcropping in the SW limit of Douro basin (Douro River mouth) and near the coastal zone south of the Douro river.	Amphibole (abundant), Apatite (accessory).
Porphyroblastic schists	Outcropping in the SW limit of Douro basin and in the littoral south of the Douro river.	Garnet, staurolite and biotite (abundant), zircon, tourmaline, apatite, sillimanite and magnetite (accessories).
Schist-greywacke complex	Outcropping mainly in the Douro and Mondego River basins.	Andalusite, garnet and staurolite (abundant in some schists and greywackes. Kyanite occasionally present.
Schists, greywacke, quartzites, hornfels and meatasediments	Outcropping mainly north of the Douro river, and present in all river basins. There are several important outcrops which are crossed by the Minho, Lima, and Mondego rivers	Biotite, andalusite in hornfels. Garnet and andalusite in schists. Apatite, tourmaline, silimanite, amphibole, pyrite, ilmenite and zircon are also present.
West Iberian Meso-Cenozoic borderland	Outcropping mainly on the Mondego, Vouga, Lis, Alcoa, and Tornada river basins.	Tourmaline, zircon and andalusite in Cretaceous formations. Andalusite, tourmaline, biotite, staurolite and zircon in Pliocene/Pleistocene deposits.

The presence of heavy minerals in the Northern Portuguese continental shelf, main river sediments and other continental sedimentary deposits is well known from several published works ([9–12,33,34]. In the Northern Portuguese rivers, from Minho to Douro rivers, and in the sedimentary filling of Minho and Douro estuaries biotite is the main transparent mineral, followed by andalusite and tourmaline. Further south in the Vouga, Lis, Alcoa, and Tornada rivers, tourmaline, andalusite, garnet, and staurolite became the dominant minerals, while in the Mondego basin sediments the most frequent minerals are tourmaline and andalusite. In the continental shelf the presence of heavy minerals is described in 5 sectors using samples collected between 10 and 120 m below mean sea level [10]. In the northernmost one (S1) the biotite is the main mineral followed by andalusite, tourmaline, zircon and garnet. In the second sector (S2) the major difference from the precedent one is the high frequency of amphibole. In the third one (S3) the principal difference from the precedent sector is the relative low frequency of biotite. The fourth one (S4) shows a similar heavy mineral distribution pattern from the precedent sector. Finally, in the fifth sector (S5) the frequency of tourmaline and andalusite represent more than 50% of the main heavy mineral assemblage (Figure 3A,B).
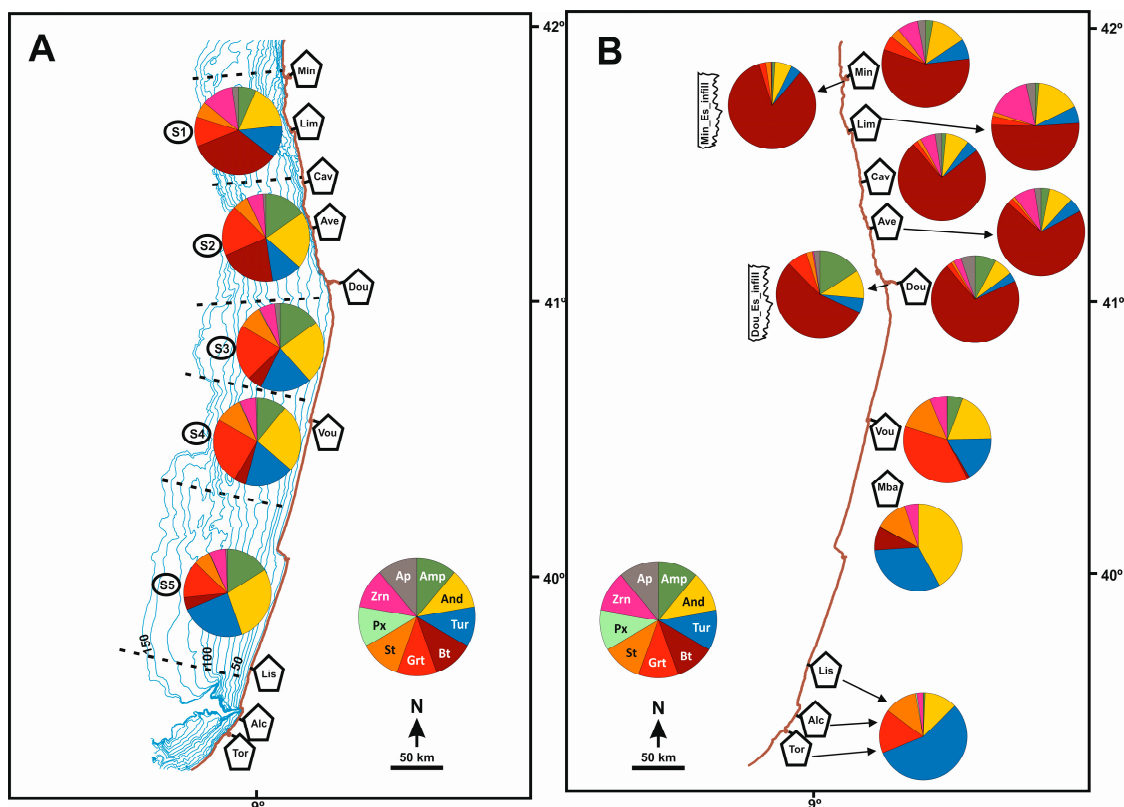
Figure 3. Heavy mineral previous data from diverse locations. (**A**) NW Portuguese continental shelf, five sectors (S1–S5). (**B**) River sediments: Minho (Min), Lima (Lim), Cávado (Cav), Ave (Ave), Douro (Dou), Vouga (Vou), Lis (Lis), Alcoa (Alc), and Tornada (Tor). Estuaries sedimentary infill: Minho (Min_Es_infill) and Douro (Dou_Es_infill). Continental sedimentary deposits: Mondego basin sediments (Mba). The heavy mineral relative frequencies were extracted from [9–11,31–34].

3. Materials and Methods

The present work is based on a set of 78 samples that were collected from three different areas of the Northern Portuguese continental margin, which match the Porto (30 samples), Aveiro (26 samples), and Nazaré (22 samples) submarine canyon upper heads (Figure 1). Samples from Porto and Aveiro areas were used for the first time in the study of heavy minerals and did not coincide with those used in previously published works that have focused on the northern part of the Portuguese continental margin [10,12]

These samples were collected during several cruises in the periods of 1990/99 and 2000/09 (Table S1) using the Smith–McIntyre grab (that collect a sediment sample with a maximum thick of 20 cm) on board hydrographical vessels (*Almeida Carvalho, NRP D. Carlos I, Andrómeda*, and *Auriga*) within the scope of the Portuguese Instituto Hidrográfico program of cartography of the continental shelf sediments (SEPLAT), Sedimentary Dynamics of the Northern Portuguese Continental Shelf project (DISEPLA II), Hotspot Ecossystem Research on the Margins of European Seas project (HERMES), and the Sedimentary Conduits of the West-Iberian Margin project (DEEPCO).

All of the samples were first washed using hydrogen peroxide and distilled water to eliminate the organic matter and marine salts. Grain-size analysis was done using the classic sieving method for sediments coarser than 4 ϕ and the settling method for finer fractions < 4 ϕ. The textural statistical parameters (mean and sorting) were computed using the method of moment [35]. Heavy minerals were separated from fine (2 ϕ) to very fine sand (4 ϕ) using bromoform in a safety laboratory equipped with an air extraction system. After this, the heavy fraction was sieved in two grain size classes: fine sand (from 2 to 3 ϕ) and very fine sand (from 3 to 4 ϕ). Each of these fractions was mounted in Canada balsam on glass slides and the required amount of heavy minerals to fill an area of 25 ×

30 mm on each slide was obtained using a micro-splitter. An average of more than 300 transparent heavy minerals per sample (considering simultaneously the two grain sizes) were counted under the petrographic microscope according to the ribbon counting method [36]. The results of the most frequent minerals (minerals with mean frequency ≥ 1%) are analyzed using the principal component analysis (PCA) based on the extraction of the correlation matrix from the initial data matrix [37]. The grain surface morphology of the most frequent heavy minerals was qualitatively evaluated under the optical microscope. For this purpose two fundamental classes were considered: angular to sub-angular and rounded to sub-rounded. When the mineral grains show little or no evidence of wear and have frequent edges, corners sharp or faces virtually untouched, they belong to the angular to sub-angular class. When the mineral grains show considerable wear, less or no original faces, edges or corners, they belong to the rounded to sub-rounded class. Using these characteristics, a visual estimative of the predominant grain morphological class in each sample was made. Additionally, to confirm the identities of heavy minerals that could be indicative of specific igneous and metamorphic sources (namely, garnet, amphibole, pyroxene, and olivine), some specific grain mounts were made using epoxy resin polished with silicon carbide (sic) and diamond polishing in polishing cloths. These grain mounts were than analyzed by an electron microprobe (JEOL Superprobe 733 at Lisbon University, Lisbon, Portugal).

The heavy mineral percentage weighted in the total sample sediment (HMwt%) was computed according to the Equations (1) and (2):

$$HM\% = \left(\frac{HMw(2-4\Phi)}{Sedw(2-4\Phi)} \right) \times 100 \tag{1}$$

$$HMwt\% = HM\% \times (Sed\%(2-4\Phi)/100) \tag{2}$$

where HM% is the weight percentage of heavy minerals in the 2–4 Φ fraction, HMw (2–4 Φ) is the heavy mineral weight (in grams) in the 2–4 Φ fraction, Sedw is the sediment weight (in grams) in the 2–4 Φ fraction, HMwt % is the heavy mineral percentage weighted in total sediment and Sed% (2–4 Φ) is the sediment weight percentage in the 2–4 Φ fraction.

4. Results

4.1. Sediment Texture (Mean and Sorting)

The mean grain size of the sampled sediments (corresponding to the 78 samples) is between 2.08 φ (fine sand; Aveiro canyon) and 3.96 φ (very fine sand; Nazaré canyon) while the sorting is between 1.58 φ (poorly sorted; Nazaré canyon) and 2.01 φ (very poorly sorted; Porto canyon) (for more details see Table S1). Additionally, the textural data reveal that the medium and fine sand are the dominant classes of the Porto and Aveiro canyon head areas, while the Nazaré canyon head area denote the presence of more heterometric sediments from very coarse sand to medium silt (Table 2).

Table 2. Average values, maximum, and minimum of mean and sorting. Values in φ units for the three canyon head areas (# = number of samples).

Canyon	#	Mean (Average)	Mean (Maximum)	Mean (Minimum)	Sorting (Average)	Sorting (Maximum)	Sorting (Minimum)
Porto	30	2.26	5.24	1.12	2.01	3.24	0.82
Aveiro	26	2.08	3.65	0.70	1.88	2.76	0.81
Nazaré	22	3.96	6.28	−0.25	1.58	3.03	0.43

4.2. Heavy Minerals Analysis

Under the petrographic microscope, it was possible to identify the presence of 18 transparent species that can be mentioned in descending order of their mean frequency in the 78 analyzed samples,

considering the sum of the two grain size classes (2–4 φ): amphibole, biotite, andalusite, tourmaline, garnets, pyroxene, staurolite, zircon, apatite, rutile, olivine, monazite, kyanite, epidote, titanite, anatase, silimanite, and brookite. The relative frequencies of these mineral grains are represented in Table 3. The results (in count values) are displayed in Table S2 as a data matrix with 78 rows (samples) and 18 columns (minerals).

Table 3. Results of the heavy mineral relative frequency for all the analyzed samples (Porto, Aveiro and Nazaré areas) considering the grain size interval between 2 and 4 φ. Mean: mean frequency for each transparent heavy mineral (values in% referred to the total transparent heavy minerals); Max: higher frequency of each transparent heavy mineral; and Min: lower frequency of each transparent heavy mineral. Heavy Minerals (HM): amphibole (Amp), andalusite (And), tourmaline (Tur), biotite (Bt), garnet (Grt), staurolite (St), pyroxene (Px), zircon (Zrn), apatite (Ap), rutile (Rt), kyanite (Ky), olivine (Ol), monazite (Mnz), epidote (Ep), titanite (Ttn), anatase (Ant), silimanite (Sil), and brookite (Brk). *HMwt*: heavy mineral percentage weighted in the total sample sediment.

	Porto			Aveiro			Nazaré		
HM	**Mean**	**Max.**	**Min.**	**Mean**	**Max.**	**Min.**	**Mean**	**Max.**	**Min.**
Amp	15.8	24.9	9.5	24.6	40.1	9.1	20.3	50.5	4.8
And	23.1	46.7	13.7	15.5	29.2	1.0	12.2	28.2	1.9
Tur	16.0	24.4	7.9	14.5	38.5	1.0	13.1	42.3	1.1
Bt	4.6	31.3	0.0	0.8	5.2	0.0	43.0	87.3	0.5
Grt	16.6	26.9	1.1	18.1	27.9	9.0	5.6	27.4	0.0
St	7.5	12.4	4.1	5.3	10.7	0.9	3.0	10.7	0.0
Px	2.1	10.3	0.0	14.0	37.8	0.2	0.0	0.0	0.0
Zrn	5.9	13.0	0.9	1.7	5.6	0.0	1.5	10.0	0.0
Ap	2.7	8.8	0.0	0.0	0.3	0.0	0.1	1.1	0.0
Rt	1.4	4.1	0.0	0.7	2.3	0.0	0.2	1.7	0.0
Ky	1.1	2.4	0.0	0.5	2.4	0.0	0.3	0.9	0.0
Ol	0.4	3.0	0.0	1.2	3.8	0.0	0.0	0.5	0.0
Mnz	0.9	3.8	0.0	0.5	1.9	0.0	0.2	0.9	0.0
Ep	0.5	1.5	0.0	0.7	3.5	0.0	0.1	0.9	0.0
Ttn	0.7	2.5	0.0	0.2	1.0	0.0	0.2	1.1	0.0
Ant	0.3	1.8	0.0	0.7	2.7	0.0	0.1	0.8	0.0
Sil	0.3	1.9	0.0	0.3	1.4	0.0	0.2	1.1	0.0
Brk	0.1	0.8	0.0	0.5	1.7	0.0	0.0	0.5	0.0
HMwt	*0.7*	*6.7*	*0.0*	*0.1*	*0.3*	*0.0*	*0.5*	*2.8*	*0.0*

4.3. Main Heavy Minerals (Porto, Aveiro, and Nazaré Areas)

The main heavy mineral suite (mean frequencies > 1%) is composed of amphibole, andalusite, tourmaline, biotite, garnet, staurolite, pyroxene, zircon, and apatite (Table 2). This mineral suite can be represented according to each studied area (Figure 4). From this figure, it is possible to observe that each area had a specific heavy mineral signature. The Porto canyon head is characterized by a main mineral suite composed, in decreasing order, of mean frequency by andalusite (23.1%), garnet (16.6%), tourmaline (16.0%), amphibole (15.8%), staurolite (7.5%), zircon (5.9%), biotite (4.6%), apatite (2.7%), and pyroxene (2.1%) (Figure 4, chart P). Aveiro contains the most representative heavy suite made up by amphibole (24.7%), garnet (18.1%), andalusite (15.5%), tourmaline (14.5%), pyroxene (14.0%), staurolite (5.3%), zircon (1.7%), biotite (0.8%), and apatite (<0.1%) (Figure 4, chart A). The Nazaré area is dominated by the presence of biotite (43.0%), amphibole (20.3%), tourmaline (13.1%), andalusite (12.2%), garnet (5.1%), staurolite (3.0%), zircon (1.5%), and apatite (0.1%). In this area, the mineral pyroxene was not identified (Figure 4, chart N).
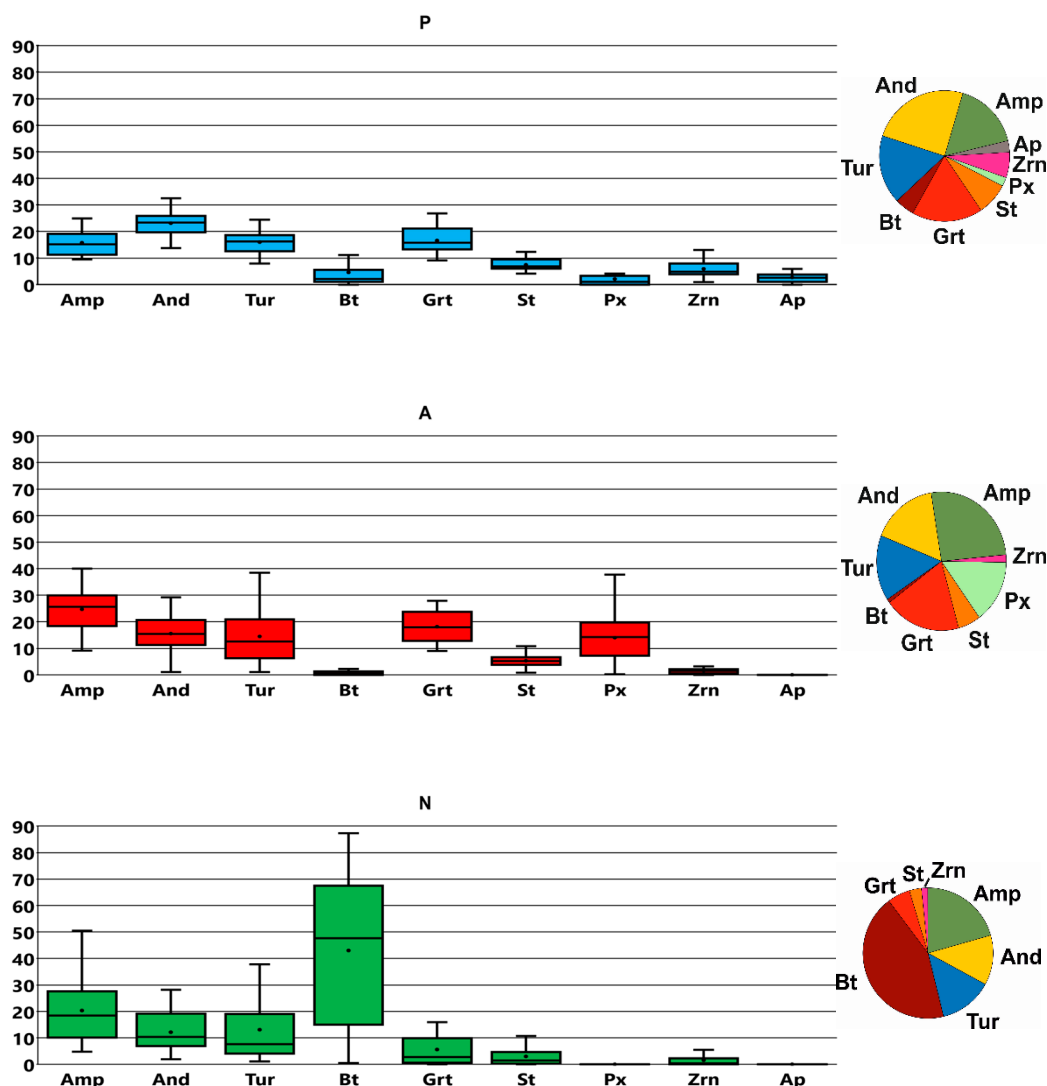
Figure 4. The heavy mineral transparent frequencies for each studied area (bar chart P—Porto; bar chart A—Aveiro; bar chart N—Nazaré) of specimens with more than 1% of mean frequency (Table 2). The box-plots represent the 25th and 75th quartiles. The horizontal line represents the 50th quartile (median). The small dots represent the mean value for each mineral. The extremes of each box vertical line represent the maximum and minimum values. Each pie chart next to the right of each bar chart represent the average frequency values of each mineral.

The distribution pattern of the main heavy mineral assemblage can be represented in detail for each studied area. In the case of the Porto area, it is verified that amphibole, andalusite, tourmaline, and garnet together represented more than 50% of the main mineral suite in all the samples. Biotite showed a high variable frequency pattern that is well represented in some samples (e.g., P22, P24, or P28) but is also absent in many samples (e.g., in most of the northernmost samples). Additionally, pyroxene tends to be more frequent in the southernmost samples, particularly in P21, P22, P23, P27, P28, P29, and P30. In a different way, zircon tend to be more frequent in the samples collected at lower depths, particularly in P1, P5, P6, P10, P16, P18, P25, P26, and P30. Staurolite and apatite show undefined distribution patterns (Figure 5).
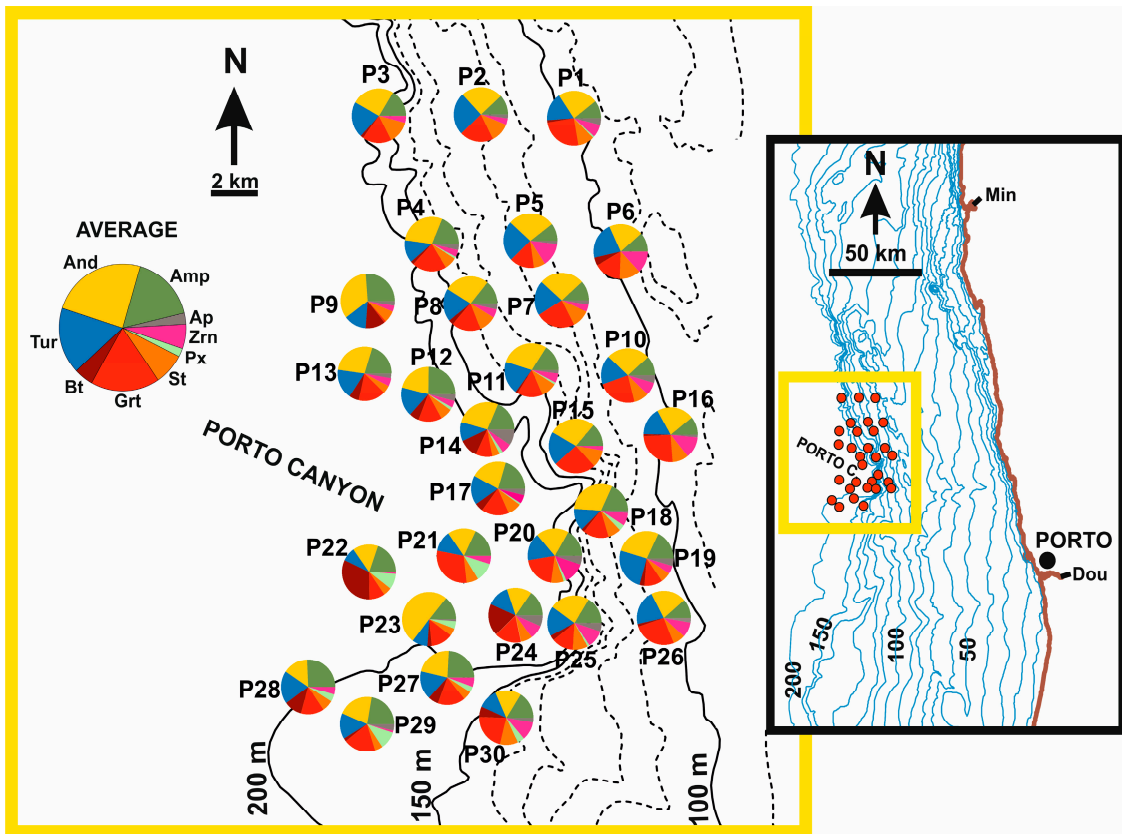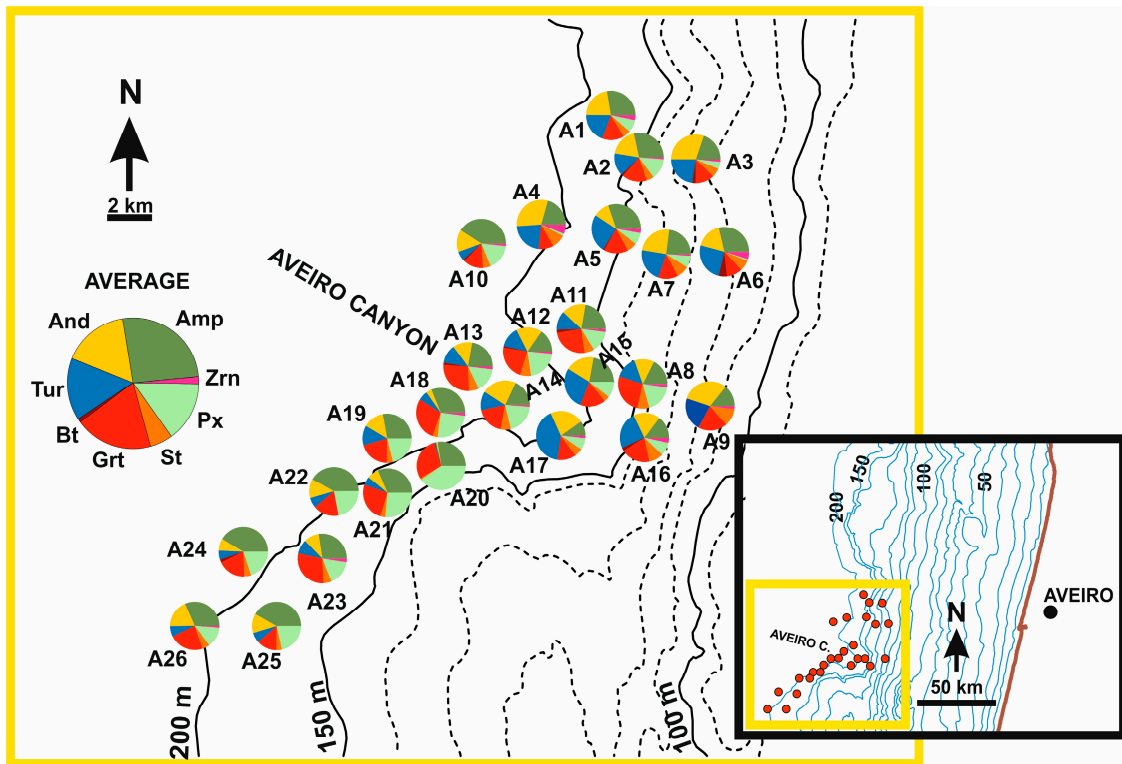
Figure 5. Main heavy mineral suite distribution according to the samples collected from the Porto upper canyon area. The average values are represented on the larger pie chart.

In the case of the Aveiro area, amphibole has a regular distribution, revealing a slight tendency to be more frequent in the southernmost samples, particularly in the A18–A24 samples. In turn, in the case of andalusite distribution, it is observed that the higher frequency values are reached in the northernmost samples (A1–A7, excluding A5), and in the ones collected along the canyon's main axis, particularly in A12, A14, and A17. Garnet is more frequent in the southernmost samples and, in contrast, tourmaline appear to be more concentrated in the northernmost samples. Pyroxene is more concentrated in the southernmost samples, representing in some cases more than 25% of the main spectrum (A20 and A21). Biotite, staurolite, and zircon are poorly represented in all the samples collected from this area (Figure 6).
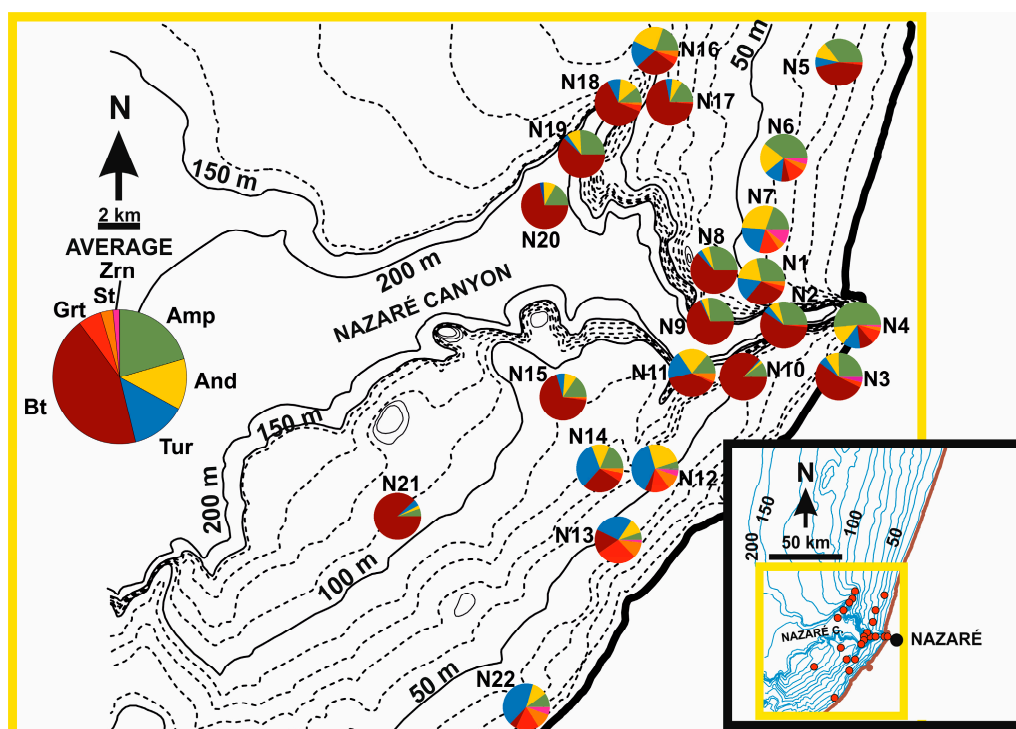
Figure 6. Main heavy mineral suite distribution according to the samples collected from the Aveiro upper canyon area. The average values are represented on the larger pie chart.

In the case of the Nazaré area, the presence of biotite is clearly dominant in most of the samples, particularly in those collected near the canyon valley where this mineral grain can represent more than two thirds of the main mineral assemblage (e.g., N9, N10, N17, N18, and N20). Amphibole seemed to be more frequent in the northernmost samples, where in some cases it can represent more than one third of the main mineral spectrum (samples N4, N5, and N6). Andalusite, tourmaline, garnet, staurolite, and zircon are more frequent in samples collected at lower depths, particularly in samples N5, N6, N7, N12, N13, N14, and N22 (Figure 7).

Figure 7. Main heavy mineral suite distribution according to the samples collected from the Nazaré upper canyon area. The average values are represented on the larger pie chart.

4.4. Principal Component Analysis

By the application of the principal component analysis (PCA) to the data matrix composed of nine heavy minerals (from amphibole to apatite) and by 78 samples it is possible to extract two components with eigenvalues higher than 1 that together explain about 65% of variance (Table 4).

Table 4. Results of the extracted principal components. Only the first two have eigenvalues higher than 1. The sum of the variance explained by the first two components is about 65%.

Component	Eigenvalue	Variance (%)
1	3.98	44.25
2	1.84	20.39
3	0.97	10.74
4	0.76	8.46
5	0.49	5.40
6	0.38	4.24
7	0.28	3.14
8	0.19	2.09
9	0.12	1.29

The first component accounts for about 44% of variance and the mineral loadings show an opposition between biotite and the mineral set composed by andalusite, tourmaline, garnet, staurolite, zircon, and apatite (Figure 8). The second component accounts for about 20% of variance and the mineral loadings on this component show an opposition between biotite and the mineral set composed by garnet and pyroxene (Figure 8).
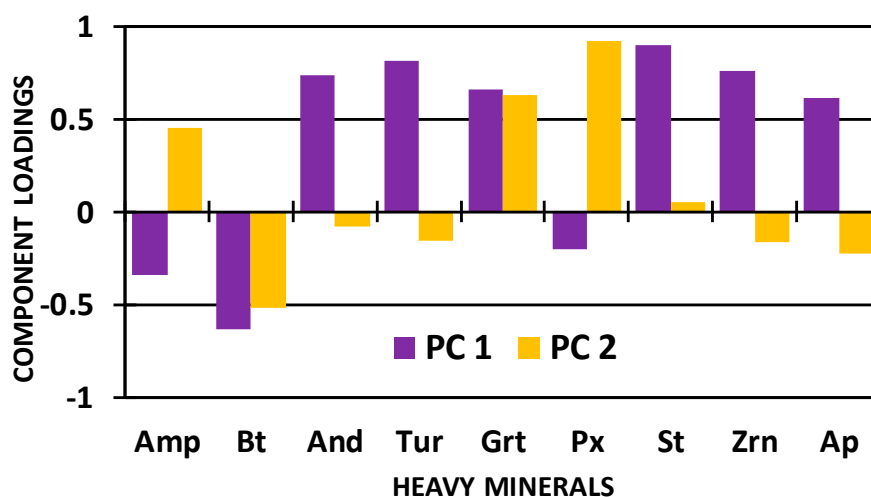
Figure 8. Mineral loadings according to the first (PC1) and second (PC2) components accounting for about 65% of variance. Amphibole (Amp), biotite (Bt), andalusite (And), tourmaline (Tur), garnet (Grt), pyroxene (Px), staurolite (St), zircon (Zrn), and apatite (Ap).

The plot of the scores of each sample considering these two principal components give rise to the scatter diagram of Figure 9. The separation of the samples according to their respective area is very clear on this diagram where the first component separates Porto samples from Nazaré samples while the second one separates the Aveiro samples from the other two sample groups (Figure 9).
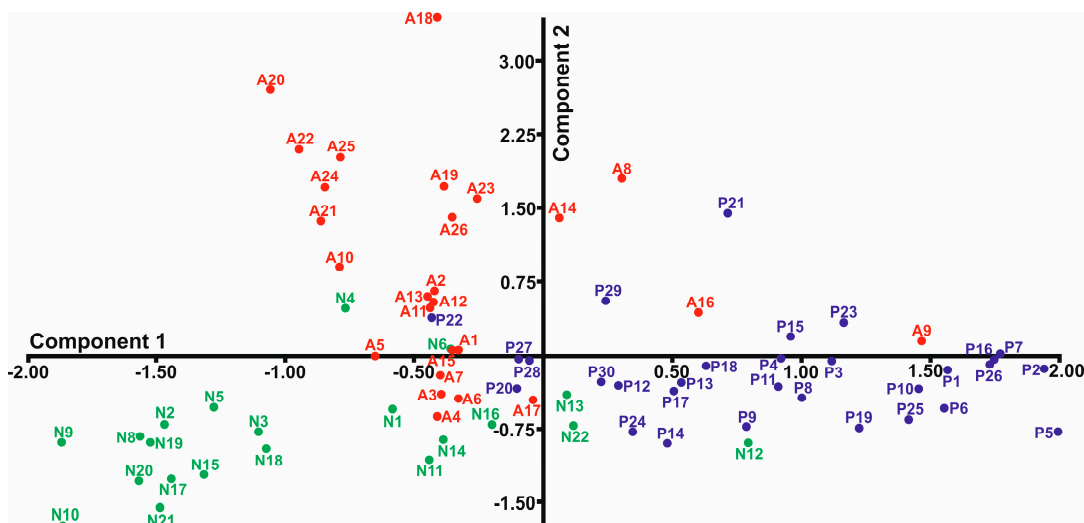
Figure 9. Scatter diagram considering the first two principal components: C1 accounts for about 44% of variance and C2 accounts for about 20% of variance.

4.5. Microprobe Analysis (Garnet, Amphibole, Pyroxene, and Olivine Mineral Groups)

The first set of heavy mineral chemical composition data it was obtained by [10]. These data correspond to samples collected from the Northern Portuguese continental shelf (Figure 10).
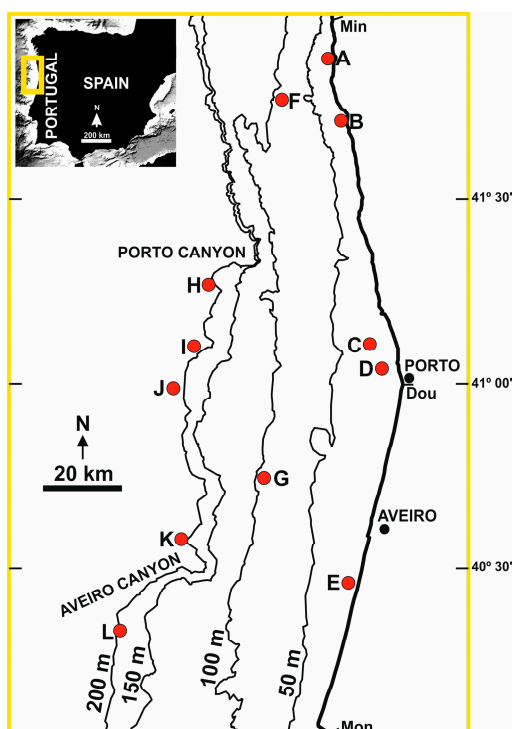
Figure 10. Location of the samples subjected to electron microprobe analysis (red dots from A–L). Min: Minho River; Dou: Douro River; Mon: Mondego River (adapted from [10]).

The second set of heavy mineral chemical composition data correspond to four samples collected from the Porto canyon head area (Figure 11).
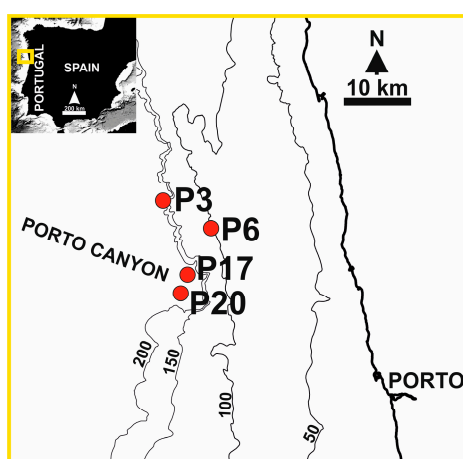

Figure 11. Location of the samples subjected to electron microprobe analysis (new data) in the Porto canyon area (red dots corresponding to samples P3, P16, P17, and P20).

4.5.1. Garnet Group

The geochemical data from detrital garnets have been used by several researchers with the aim of interpreting the sedimentary provenance [38–42]. This mineral group is known for its potential in the analysis of the sedimentary provenance of detrital sediments because "it has a wide compositional variation that may be specific to certain lithologies and, therefore, source areas, it is mechanically resistant during transport, and it is resistant to chemical modification during transport, diagenesis and low-grade metamorphism" [42] (p.373). All the available data corresponding to the microprobe

analysis of detrital grains of garnet are shown in Figure 12A,B). This figure was built using the excel spreadsheets made available by [42,43] and following the recommendations of [43].
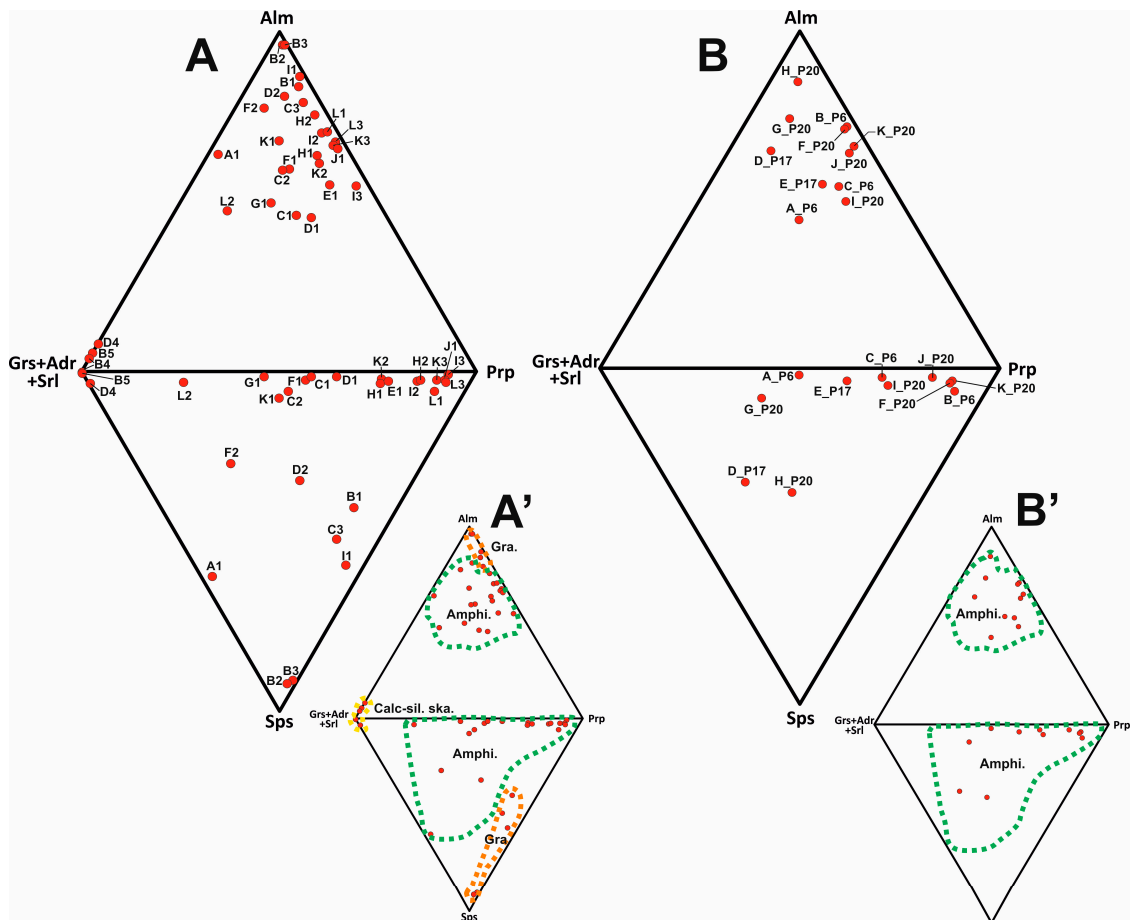

Figure 12. Ternary plots using end-members grossular (Grs) + andradite (Adr) + schorlomite (Srl), almandine (Alm), pyrope (Prp), and spessartine (Sps). **A** shows the results corresponding to several samples collected from the Northern Portuguese continental shelf (first set of chemical composition data obtained by [10]). The capital letter next to each red dot indicates the location of the sample on the map of the Figure 10. The number next to the capital letter is the reference to the analyzed mineral grain. **B** shows the results corresponding to the second set of heavy mineral composition data (samples collected from the Porto canyon head area). In this case the capital letters represent each analyzed mineral grain. Each sample is referenced by the letter P followed by a number. The location of the samples is shown in Figure 11. **A'** and **B'** are the ternary plots showing sub-areas characteristic of garnets with different protoliths: Gra—granites, Amphi—amphibolites, Calc-sil. ska—calc-silicate skarns.

The results of the ternary plot of Figure 12A show the predominance of garnets with the dominant presence of the almandine end-member. However, a small number of samples (B4, B5, and D5) show the predominance of the grossular (Grs) + andradite (Adr) + schorlomite (Srl) end-member. The protoliths corresponding to the analyzed garnets can be observed in Figure 12A'. Figure 12B shows only the predominance of the almandine end-member and the correspondent protoliths can be observed in Figure 12B' (see Table S3 for details).

4.5.2. Amphibole Group

The classification of these amphiboles is made according to the spreadsheet of [44] that follows the nomenclature recommended by the International Mineralogical Association [45]. The chemical composition of the analyzed amphiboles is plotted according to the diagrams defined by [46]. For

the samples collected from the Northern Portuguese continental shelf [10] (Figure 10) the presence of magnesio-hornblende (Mhb) is predominant (it is detected in 14 samples). Other types of calcic amphiboles are tschermakite (Ts), edenite (Ed), pargasite (Prg) (all detected in three samples), ferro-hornblende (Fhb) detected in two samples, and finally actinolite (Act), magnesio-hastingsite (Mhst), and hastingsite (Hst) (all detected only in one sample) (Figure 13A,B; see Table S4 for details).
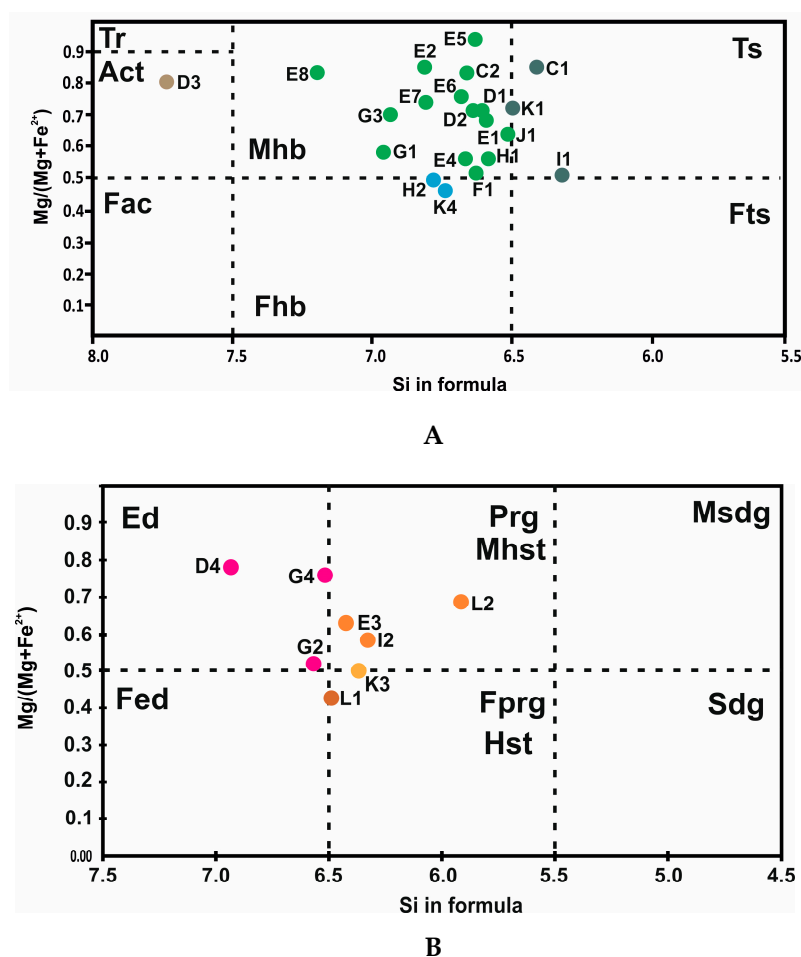

A

B

Figure 13. A (upper diagram) shows the presence of magnesio-hornblend (Mhb), tschermakite (Ts), ferro-hornblende (Fhb) and actinolite (Act). In this diagram tremolite (Tr), ferro-actinolite (Fac) and ferro-tschermakite (Fts) were not found. **B (lower diagram)** shows the presence of pargasite (Prg), edenite (Ed), magnesio-hastingsite (Mhst), and hastingsite. In this diagram ferro-edenite (Fed), magnesio-sadanagaite (Msdg) and sadanagaite (Sdg) were not found. The capital letters next to each dot indicates the location of the sample on the map of the Figure 10. Each number next to each capital letter is the reference of the analyzed mineral grain. These diagrams project chemical analysis data of calcic amphiboles from samples collected from the Northern Portuguese continental shelf.

For the samples collected from the Porto canyon area (Figure 11) the analyzed amphiboles belong to the group of calcic amphiboles. The presence of magnesio-hornblende (Mhb) is predominant (detected in 11 samples), followed by tchermakite (Ts) (in three samples), pargasite (Prg) (in three samples), and by ferro-tschermakite (Fts) and actinolite (Act) both detected in one sample (Figure 14A,B; see Table S4 for details).
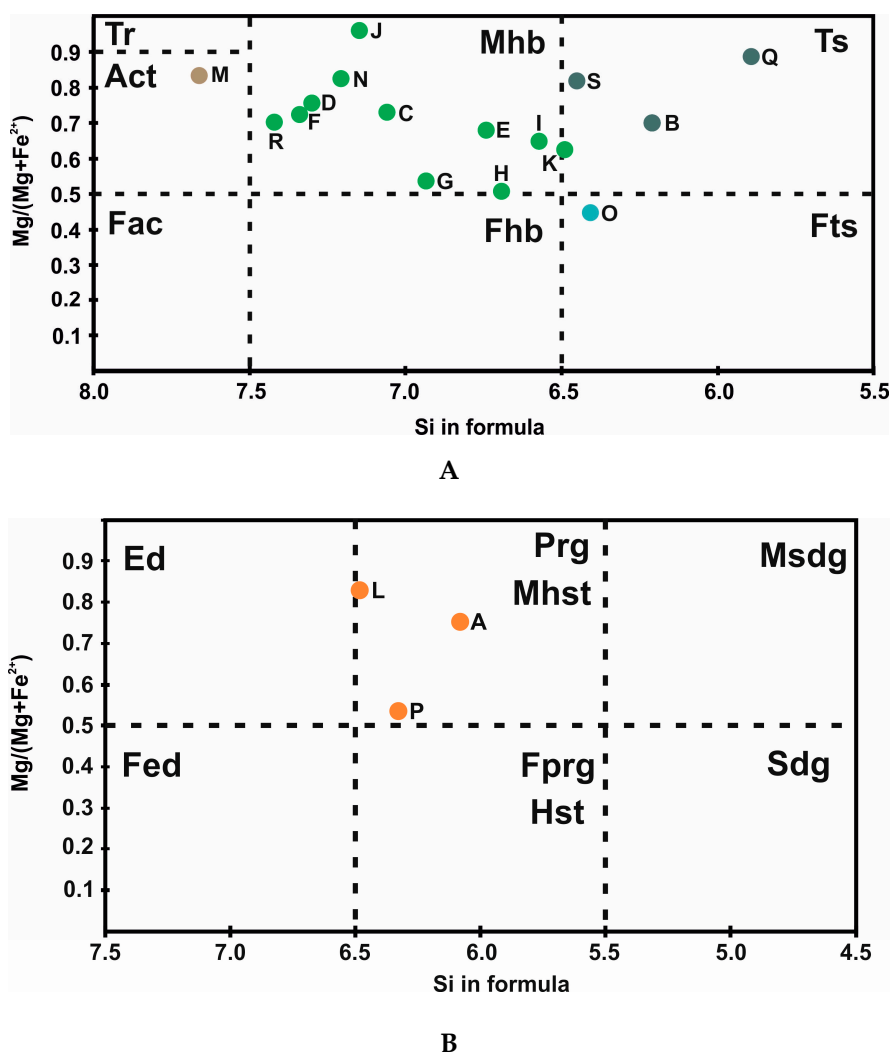
A

B

Figure 14. **A (upper diagram)** shows the presence of magnesio-horneblend (Mhb), tschermakite (Ts), ferro-tschermakite (Fts) and actinolite (Act). In this diagram tremolite (Tr), ferro-actinolite (Fac), ferro-hornblend (Fhb) were not found. **B (lower diagram)** shows the presence of pargasite (Prg). In this diagram edenite (Ed), magnesio-hastingsite (Mhst), hastingsite (Hst) ferro-edenite (Fed), magnesio-sadanagaite (Msdg), and sadanagaite (Sdg) were not found. Mineral grains D–N are from sample P6; A–C are from sample P3; P–S are from sample P20; O is from P17. The location of the samples can be seen on Figure 11. These diagrams project chemical analysis data of calcic amphiboles from samples collected from the Porto canyon area.

4.5.3. Pyroxene Group

The classification of the pyroxenes is made using the available spreadsheet by [47] and the results were plotted according to the ternary diagrams defined by [48]. For the samples collected from the Northern Portuguese continental shelf [10] and considering the group of clinopyroxenes it is possible to detect the presence of diopside (Di) in five samples, of hedenbergite (Hd) in seven samples, and of augite (Aug) in three samples. For the orthopyroxene group it is possible to detect the presence of enstatite (En) in seven samples, and ferrosilite (Fs) in two samples (Figure 15; see Table S5 for details).
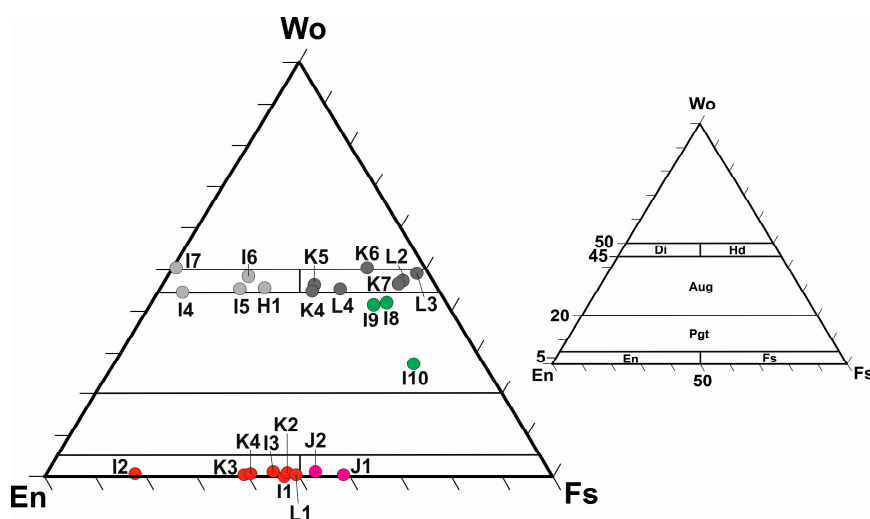
Figure 15. Classification diagram for identified pyroxenes in samples collected from the Northern Portuguese continental shelf by combining the classification diagrams of clinopyroxenes and orthopyroxenes proposed by [48]. The classification shows the presence of diopside (Di), hedenbergite (Hd), augite (Aug), enstatite (En), and ferrosilite (Fs). Pigeonite (Pgt) was not found. The capital letters next to each dot indicates the location of the sample on the map of the Figure 10. Each number next to each capital letter is the reference of the analyzed mineral grain.

For the samples collected from the Porto canyon area and considering the group of clinopyroxenes it is possible to detect the presence of diopside (Di) in five samples, of hedenbergite (Hd) in one sample, and of augite (Aug) in six samples. For the orthopyroxene group it is possible to detect the presence of enstatite (En) in four samples, and ferrosilite (Fs) in two samples (Figure 16; see Table S5 for details).
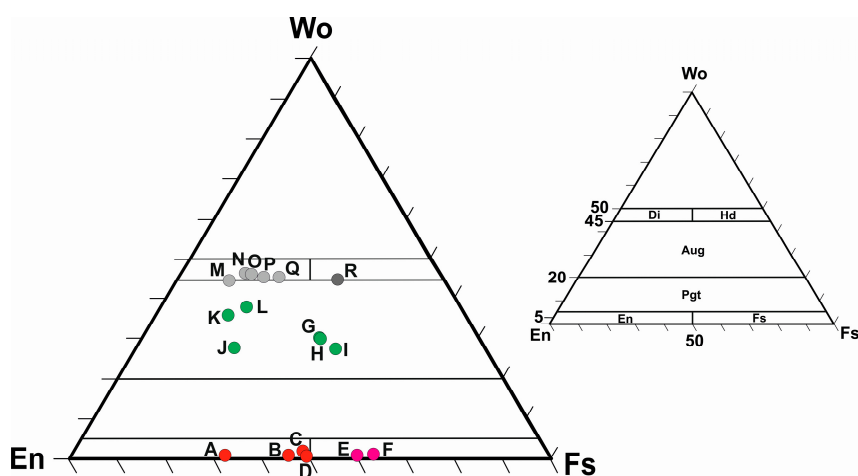

Figure 16. Classification diagram for identified pyroxenes in samples collected from the Northern Portuguese continental shelf by combining the classification diagrams of clinopyroxenes and orthopyroxenes proposed by [48]. The classification shows the presence of diopside (Di), hedenbergite (Hd), augite (Aug), enstatite (En), and ferrosilite (Fs). Pigeonite (Pgt) was not found. A–D are En mineral grains from sample P20; E and F are Fs mineral grains from sample P20; G–I are Aug mineral grains from sample P6; J and K are Aug mineral grains from sample P17; L is a Aug mineral grain from sample P20. The location of the samples can be seen on Figure 11.

4.5.4. Olivine Group

The classification of the olivine is made using the available spreadsheet by [47] and the results are plotted using a diagram expressing the compositional variation between the two extreme members:

forsterite (Fo) and fayalite (Fa). For the samples collected from the Northern Portuguese continental shelf it is possible to detect two olivine mineral grains with strong composition in Fo end-member (Figure 17A,A'; see Table S6 for details).
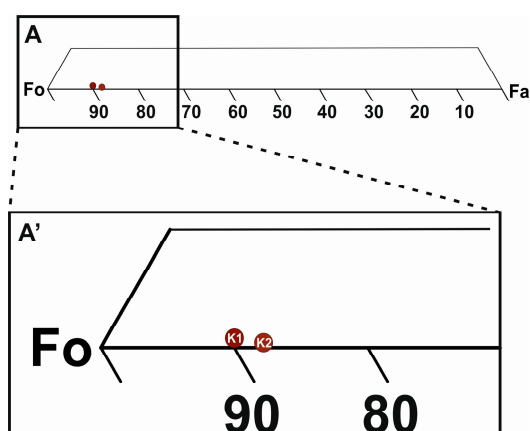

Figure 17. Classification diagram of identified olivine's in samples collected from the Northern Portuguese continental shelf. The capital letters inside to each dot indicates the location of the sample on the map of Figure 10. Each number next to each capital letter is the reference of the analyzed mineral grain. In A', it is possible to observe that the Fo end-member has a value greater than 85%.

For the samples collected from the Porto canyon area the strong presence of the Fo end-member is also found (Figure 18A,A').
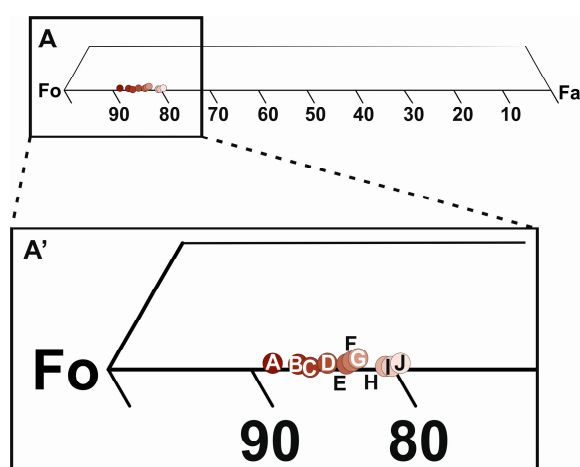

Figure 18. Classification diagram of identified olivines in samples collected from the Porto canyon area. A, D, and G are Fo mineral grains from sample P20; B, C and J are Fo mineral grains from sample P3; F and H are Fo mineral grains from sample P17; E is a Fo mineral grain from sample P3. In A', it is possible to observe that the end member Fo ranged between 80 and 90%.

4.6. Mineral Grain Surface Morphologies

The most common transparent heavy minerals identified under the optical microscope appear with contrasting morphological surface morphologies. Two fundamental classes of surface morphologies are considered: angular to sub-angular and rounded to sub-rounded. The first class includes heavy minerals correspondent to "first-cycle" particles independently from their source. These minerals can be found in all the samples analyzed and they are dominant (>50%) in samples collected from the three studied areas at depths exceeding 120 m. The second class includes heavy minerals that show a long evolution in the sedimentary environment and for that reason they can be considered as "multi-cycle" particles. These minerals are dominant (>50%) in samples collected from the three studied areas at

depths of less than 120 m (Figure 19). In this figure the heavy-mineral classification is based on the description of the minerals surficial textures referred by [49,50]

Figure 19. Typical visual aspects of the main heavy mineral transparent suite according to their dominant surface texture. Mineral grains classified with *first-cy.* are "first-cycle" particles that have angular to sub-angular surface textures and are catalogued with odd numbers from 1–15 and continuously from 17–22. In this class it was detected the presence of several euhedral Fo minerals (grain 21). Mineral grains classified with *multi-cy.* (catalogued with odd numbers from 2–16) correspond to the "multi-cycle" ones.

5. Discussion

5.1. Heavy Mineral Sources

One can verify that a correlation exists between the presence of the main heavy mineral assemblage made of amphibole, andalusite, tourmaline, biotite, garnet, staurolite, zircon, and apatite with the fluvial heavy mineral spectrum formerly identified in the Northern Portuguese river basins (Figures 4 and 6–8) [31–34]. Furthermore, this mineral assemblage is also compatible with the igneous and metamorphic rocks that appear in these river basins, which can be considered as primary sources of these heavy minerals (Figure 3 and Table 1). Thus, it is possible to cite the examples of andalusite-rich metamorphic rocks as important sources of andalusite, of porphyroblastic schists known as main sources of garnet, staurolite, and biotite, of micaschists, gneisses, and granites identified as important sources of biotite, tourmaline, apatite, and zircon, as well as amphibolites of the Douro metamorphic complex known as main sources of amphibole [30].

The two sets of microprobe analysis results (Figures 12–18) make a strong mineral-chemical tool to determine heavy mineral provenance. In this context, the garnets from the Northern Portuguese continental shelf that were analyzed show a source compatibility with granites, with intermediate to high-grade metamorphic rocks (of amphibolitic and granulitic facies), and with calc-silicate skarns. This interpretation is based on the relationship between the sub-area's characteristic of garnets with the different protoliths referred by [42] (Figures 12A and 20A). The garnets compatible with granites are mostly found in samples collected at low depths north of the Douro River (samples B and C, Figure 10). This means that the main outcrops of granites present at Minho, Lima, Ave, and Cávado river basins (Figure 2 and Table 1) are the most likely primary sources of these garnets. However, in a sample collected from the upper continental slope, between Porto and Aveiro canyon areas (sample I, Figure 10), the presence of one garnet compatible with this granitic source was detected. The garnets sourced from metamorphic rocks (of amphibolitic and granulitic facies) are found throughout the Northern Portuguese continental shelf (samples A to L, Figure 10). The occurrence pattern of these garnets certainly reflects the widespread presence of metamorphic rocks (of amphibolitic and granulitic facies) all over the Northern Portuguese river basins (Figure 2 and Table 1). The presence of grossular end-member rich garnets (with more than 80% in grossular composition; Table S3) is confined to two samples collected at low depths (samples B and D, Figure 10). According to the parameters of [42] these garnets can be sourced from "calc-silicate skarns and rodingites". The most important Portuguese calc-silicate skarn deposits are found in the central-northern part of the country (Central Iberian Zone). These deposits are within the Dúrico-Beirão Supergroup lithostratigraphic sequences [51]. Of these occurrences it is possible to highlight the presence of skarns at the mining districts of Covas (Minho region) and Tabuaço (Douro river basin) where the presence of grossular is known [52,53]. Thus, it is possible to conclude that these kinds of garnets (rich in grossular end-member) have, for their main primary sources, these skarn deposits present in the Douro, Lima, and Minho river basins (Tabuaço and Covas areas). In regard of the chemical composition of garnets concerning the second sample set (samples collected from the Porto canyon area), the results only show a source compatibility with metamorphic rocks of amphibolitic and granulitic facies (Figures 12B and 20B), based on the parameters defined by [42]. Since these rocks are well represented in the Douro river basin (as the most important group of metamorphic rocks; Figure 2 and Table 1) it is possible to conclude that these garnets were essentially sourced from the Douro river basin.
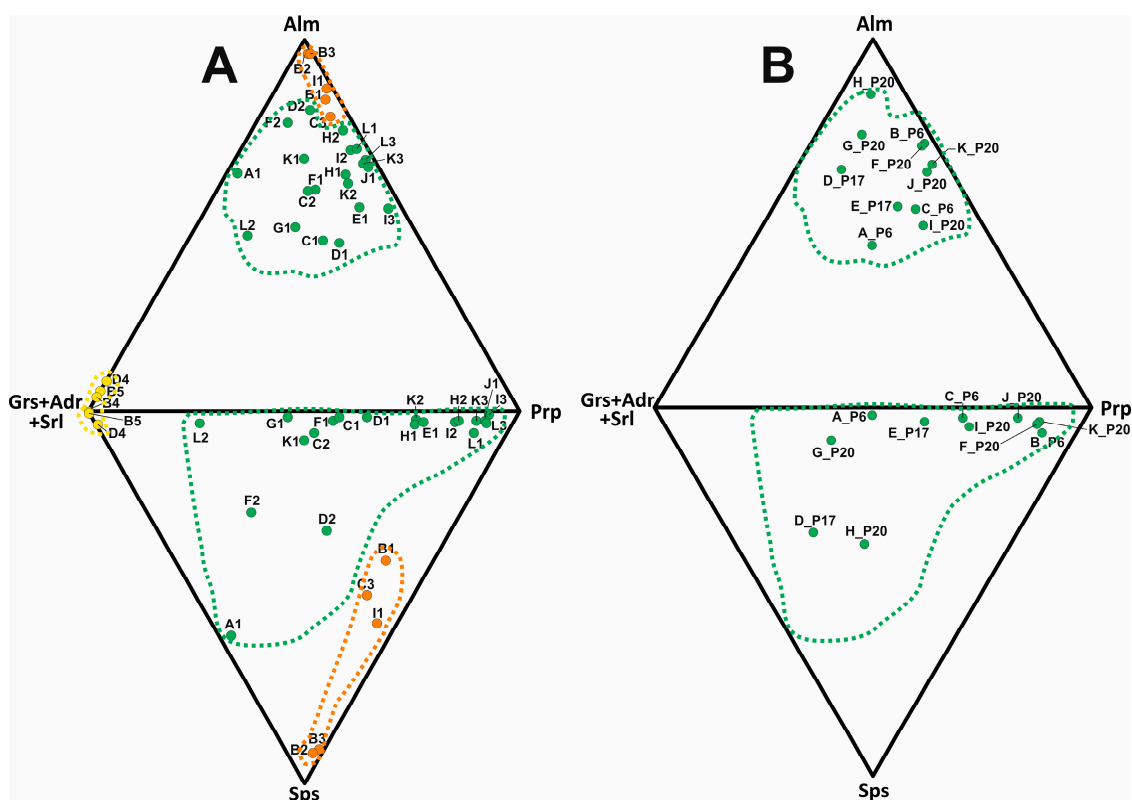
Figure 20. (**A**). Northern Portuguese continental shelf. Orange dots and correspondent surrounding area indicate garnets sourced from granites. Green dots and correspondent surrounding area indicate garnets sourced from metamorphic rocks of amphibolitic and granulitic facies. Yellow dots and correspondent surrounding area represent garnets sourced from calc-silicate skarns. (**B**) Porto canyon area. Green dots indicate garnets sourced from metamorphic rocks of amphibolitic and granulitic facies.

For the first sample set (samples collected from the continental shelf), the available data on the amphibole chemical composition show the predominance of magnesio-hornblende, followed by other calcic amphiboles, such as tschermakite, edenite, pargasite, ferro-hornblende, actinolite, magnesio-hastingsite, and hastingsite (Figure 13A,B). The most likely sources for these amphiboles are the amphibolitic rocks of the Douro metamorphic complex (Figure 2 and Table 1). However, among the mineral grains with pargasite composition, two grains with a relatively high content in TiO_2 (I2 with 2.0% and L2 with 3.4%; Table S4) were detected. Under optical microscope observation, in plane polarized light, these amphiboles appear with shades of brown which makes them easily distinguishable from other amphiboles (Figure 19, mineral #17). These cases of pargasite may be indicative of a provenance related to basic igneous rocks, such as gabbro [54]. Similar source interpretation can be considered for the presence of the magnesio-hastingsite (mineral grain K3; Figure 13A) detected near the Aveiro canyon area (Figure 10). As these amphiboles were only found in the deepest areas of the continental shelf, south of Porto canyon (samples I, K and L, Figure 10), and knowing that this igneous basic source is not represented in the Northern Portuguese river basins, then it will be necessary to admit the existence of a compatible source located elsewhere in the outershelf/upper slope south of Porto canyon. For the second sample set (samples collected from the Porto canyon area), the available data of the amphibole chemical composition show the dominant presence of magnesio-hornblende (Figure 14A). The provenance of these amphiboles is compatible with the amphibolitic rocks of the Douro metamorphic complex (Figure 2 and Table 1). In this sample set it is also identified the presence of pargasite in three samples with relatively high values of TiO_2 (between 0.9 and 1.4%, Figure 14B and Table S4). Moreover, these pargasite mineral grains appear with shades of brown under the microscope observation in plane polarized light (Figure 19, mineral #17). Therefore, these data point to the fact

that these amphiboles have an origin related with basic igneous rocks as discussed above. The source of the other identified amphiboles (actinolite, tschermakite, and ferro-tschermakite) is compatible with the metamorphic rocks outcropping in the referred river basins (Figure 2 and Table 1). For a better understanding the relationship between the identified amphiboles and their most typical sources, Table 5 makes the synthesis of the results referent to this mineral group.

Table 5. Correspondence between the identified amphiboles, most typical primary sources and sample sets. 1st—first set of heavy mineral chemical compositional data (Northern Portuguese continental shelf). 2nd—second set of heavy mineral compositional data (Porto canyon head area). Mhb—magnesio-hornblende, Act—actinolite, Ts—tschermakite, Fts—ferro-tschermakite, Fhb—ferro-hornblende, Ed—edenite, Prg—pargasite, Mhst—magnesio-hastingsite, Hst—hastingsite.

Amphibole	Typical Primary Sources	Sample Set
Mhb	amphibolite, schist	1st; 2nd
Act	metamorphized carbonate rocks	1st; 2nd
Ts	amphibolite	1st; 2nd
Fts	amphibolite, schist, gneiss	2nd
Fhb	amphibolite, schist	1st; 2nd
Ed	amphibolite	1st; 2nd
Prg	gabbro; amphibolite, schist, calc-silicate skarns	1st; 2nd
Mhst	alkali basalts	1st
Hst	amphibolite, schist, granite, gneiss	1st

The presence of pyroxene and olivine mineral grains in the deeper areas of continental shelf around Porto and Aveiro canyons areas is not compatible with the felsic igneous and metamorphic rock outcroppings in the Northern Portuguese river basins, since these mineral grains are genetically linked to basic igneous rocks such as basalt, gabbro, or dolerite [55], whose presence is not known in these river basin areas (Figure 2 and Table 1). The first reference to these mineral grains in the Northern Portuguese continental shelf describes the occurrence of "augite" and "hypersthene" in a restricted area located south of the Porto canyon, at depths greater than 100 m [56]. In this work, a source interpretation was outlined which emphasized the existence of basic igneous rocks near this canyon head area, given the fact that these mineral grains have always fresh and angular surface textures which demonstrates their incompatibility with a multi-cycle source as for example from an ancient shoreline, that is, from a relict or palimpsest continental shelf deposits. The optical identification of pyroxenes (mineral grains #18 to #20; Figure 19) is confirmed by the microprobe analysis of several mineral grains belonging to the two samples sets. The chemical composition of pyroxenes shows the presence of some mineral grains compatible with the diopside-hedenbergite and enstatite-ferrosilite series composition, and with augite composition (Figures 15 and 16). It turns out that the optical identification of olivine (mineral grains #21 and #22; Figure 19) is also confirmed by the microprobe analysis of several mineral grains belonging to samples collected from the continental shelf and from the Porto canyon areas, revealing a high content in forsterite end-member (Figures 17 and 18). At the same time, the existence of a seismic reflection profile complemented by bathymetric data and images of the sea floor captured by a remote operated vehicle (ROV), detected the presence of a geological structure near the Porto canyon head area (Figure 21A) with a probable volcanic origin [13,57]. This structure was described as a rock relief more than 15 m height, standing out from neighboring geological formations and it was recognized in a seismic profile by a very distinctive diffractive hyperbola (Figure 21B,C). Its presence was attributed to a hard rock body (of limestone to dolomitic nature) that stood out from the nesting sedimentary rocks (detrital sediments with evidence of carbonate cement). This rock body seems to be embedded in a fault zone that shows evidence of relative movement between the two adjacent blocks; the WSW block has lowered about 2.5 m relative to the ENE block (Figure 21D). During a ROV dive, it was possible to confirm that the referred rock body was made of dolomitic rocks showing signs of karstic erosion [13]. Indirect evidence for the existence of volcanic rocks was found inside

this dolomitic structure due to the presence of an elongated depression (with an approximate N–S direction) that could be a match for a volcanic dyke that is now completely eroded [13].
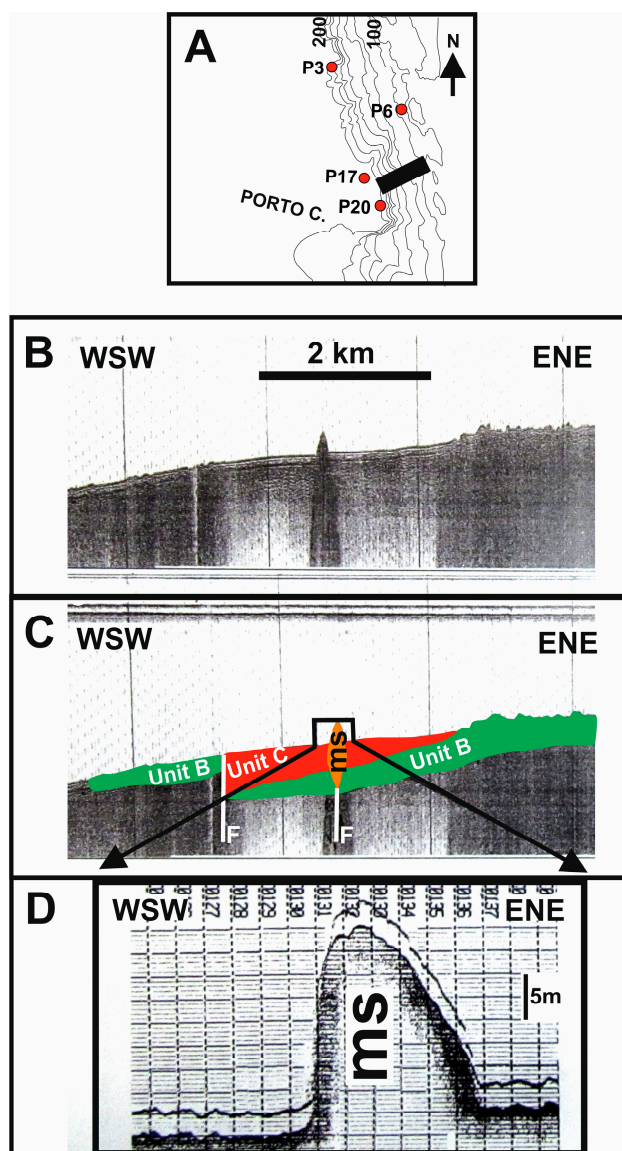

Figure 21. (A–D). Seismic reflection profile obtained at the Porto canyon head latitude. (**A**) Localization of the profile; (**B**) Seismic profile without interpretation; (**C**) interpreted seismic profile with localization of the metamorphic structure (ms); and (**D**) Detail of the bathymetric profile of the metamorphic structure. F corresponds to the interpreted faults. Unit B corresponds to a Mesozoic rock unit. Unit C corresponds to a Cenozoic rock unit (interpreted as dolomitized detrital limestones). Adapted from [13].

All the available data concerning to the optical characteristics and the chemical composition of diopside-hedenbergite, augite, enstatite-ferrosilite, fosrterite, pargasite rich in Ti, and magnesio-hastingsite mineral grains allow to sustain that this mineralogical assemblage is exclusively represented in the areas around the Porto and Aveiro canyons (Figures 13B, 14B and 15, Figures 16–18). Within this mineral assemblage it is possible to distinguish the influence of two different main sources. While augite and enstatite-ferrosilite could be sourced from igneous basic rocks, the presence of diopside-hedenbergite and forsterite may be derived from metasomatic processes resulting from chemical reactions between an igneous basic rock with the nesting sedimentary rocks (limestones and dolomites) [58]. During these processes, the circulation of fluids in the limestone-dolomitic

formations and the high temperature inherent to the installation of the volcanic body could explain the formation of these specific minerals, as their presence is referred in other geological contexts associated with the formation of magnesian and/or calcic skarns [59,60]. References to the presence of detrital forsterite with euhedral shapes as it is detected in some of the studied samples (mineral grain #21; Figure 19) are not easy to find in the literature. However, in a different geological context, the presence of euhedral Fo (among other minerals) can be interpreted as a result of re-crystallization processes during contact metamorphism between igneous basic rocks (gabbro) and dolomitic limestones [61]. Therefore, with all due precautions and based on the existing data, it is possible to consider that the presence of this specific mineral assemblage (diopside-hedenbergite and forsterite) is probably related with metasomatic process derived from the thermal contact between basic igneous rocks and dolomitic limestones (possible formation of calcic and magnesian skarn rocks). Together, these rocks (basic igneous and dolomitic limestones affected by metasomatic processes) can be considered as local sources.

5.2. The Nazaré Canyon Area

For the specific case of the Nazaré area, the dominant presence of biotite, followed by amphibole, tourmaline, andalusite, and garnet (Figures 4N and 7) calls for a specific interpretation from the point of view of mineral source and physical grain sorting. According to available data, the high frequency of biotite (>40%—Figure 7) only occurs when the sediment has a mean grain size higher than 2.5 ϕ, that is, when the presence of fine sand to very coarse silt is dominant (Table S1). Moreover, when the biotite frequency is extremely high (biotite > 50%) the sediment mean grain size is equal or higher than 2.5 ϕ (Figure 22). This is consistent with the fact that mica flakes are preferentially concentrated in the coarser part of the sediment tail because of their lamellar shape, that is, they are hydraulically equivalent to finer-grained sediments [62]. Considering that the most proximal sources of heavy minerals are depleted in biotite as it can be observed in the continental shelf sector S5 and in Lis, Alcoa and Tornada river sediments (Figure 3), this high concentration of biotite could result from hydrodynamic fractionation (mineral grain sorting). This can only be understood in the context of a long transport path from a distal source (Northern Portuguese river basins) to the main depocenters located on this canyon head area (Nazaré). This interpretation is supported by the heavy mineral composition of the Minho to Douro river sediments where biotite is, by far, the most important heavy mineral (Figure 3). Thus, the biotite sorting may occur in several steps. The first sorting affects the original source (the Portuguese northern river input) when sand particles are selectively transported from the river into the inner shelf domain [12]. The second step occurs during the inner shelf southward transport of fine sand [63] and, finally, the third step happens when only the finer (and lamellar) sand particles are captured and temporary deposited on the canyon upper head valleys according to the complex oceanographic processes that take place in this area [15,16,63,64]. Given that biotite flakes are hydraulically equivalent to fine grained sediments, their resuspension could happen during the typical oceanographic regimes that affected the Nazaré canyon area [16]. During summer sediments are laterally transported in suspension into the canyon during the upwelling regime, and the resuspension of fine sediments present in the mid-shelf deposits happens due to the internal wave's activity. Additionally, during this regime, the sediments transported through the north-south littoral drift are captured in the head of the canyon. During the winter regime fine sediments captured by the canyon are essentially sourced from southern rivers and from southern continental shelf. When these sediments are sourced from the continental shelf they are resuspended and transported by the combined effect of the waves and the poleward current that is established during the downwelling regime [14–16]. Thus, the high concentration of this mineral found in most of the Nazaré samples is related to how easy it is for biotite to be transported in suspension due to its lamellar shape, which is a characteristic that makes it hydraulically equivalent to finer sedimentary particles. This interpretation agrees with the knowledge of the hydraulic behavior of mica flakes in sand sediments known since the 1960s [65–69].
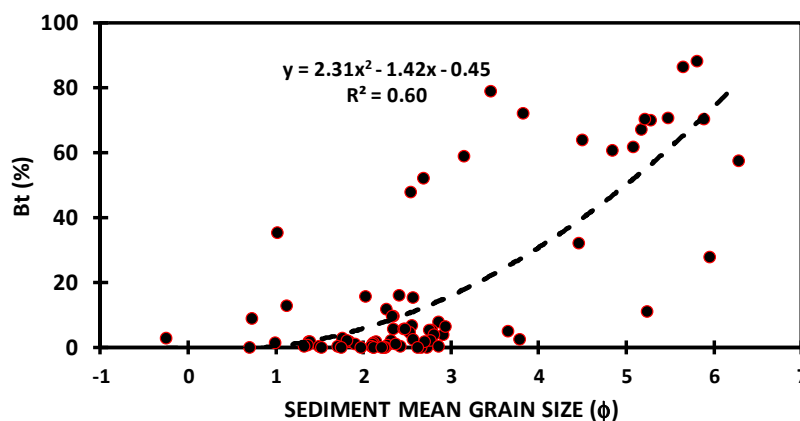
$$y = 2.31x^2 - 1.42x - 0.45$$
$$R^2 = 0.60$$

Figure 22. Correlation between biotite frequency and sediment mean grain size using a polynomial function of degree 2.

5.3. The Meaning of the PCA Results

It is possible to observe in the scatter diagram of Figure 9 regarding the application of PCA that there is a clear separation of the samples according to the area from where they were collected. The comparison of the samples position in the scatter diagram (Figure 9) with their respective geographical location visible in Figures 5–7 is quite straightforward. For example, concerning the Aveiro area, samples that are further away from the center of the diagram of Figure 9 (A18–A26) are present in the extreme SW of the sampled area (Figure 6). They also have in common the high frequency of pyroxene (Figures 6 and 9). For Porto samples, no correlation between the way the samples are placed on the scatter diagram (Figure 9) and their respective geographical position exist (Figure 5). However, samples P21, P22, and P29 can be considered exceptions as they were collected from the SW part of the sampled area (Figure 5). These samples together with the correspondent ones collected from the Aveiro area have in common the relative high frequency of pyroxene. Thus, the influence of the igneous basic local source seems to be more distinct on both most southwestern samples collected from Porto and Aveiro canyon areas. Regarding Nazaré, the samples that are further away from the center of the Figure 9 diagram (N2, N3, N5, N8, N9, N10, N15, N17, N18, N19, N20, and N21) have in common the high frequency of biotite. The position of these samples will then correspond to the sites where sediment resuspension phenomena is more frequent.

5.4. The Interpretation of the Heavy Mineral Grain Surface Morphologies

The presence of mineral grains with contrasting surface morphologies, from the most angular to the most rounded ones (Figure 19), could be indicative of potential sources diversity, transport pathways, and sediment deposit's nature. Previous studies dealing with the presence of heavy minerals in the Northern Portuguese continental shelf have considered that the mineral grains with "predominantly rounded to sub-rounded forms" suggest a "polycyclic origin or a long exposure to dynamic processes prior to deposition" [12]. These mineral grains make a contrast with the presence of more angular mineral ones that are believed to be delivered more directly from primary sources (felsic igneous and metamorphic rocks) [12]. The presence of rounded mineral grains is more common in the outer shelf at depths less than 120 m in the three studied areas, and their presence suggests a "multi-cycle" sedimentary origin compatible with long exposure to dynamic processes, which are typical of high energy environments such as, for example, beach environments where the intense grain abrasion is frequent [70]. Although most of these rounded mineral grains were found at the referred depths, some of them are found at the shelf break and in the upper slope (depths >140 m), which could be happening due to of some particle remobilization and transportation into deeper areas. This means that the presence of such mineral grains could be suggestive of a source corresponding related with reworked sedimentary shelf deposits, namely the medium to coarse sand deposits present on this continental

margin at depths between 60 and 100 m genetically linked to ancient littorals (relict sediments) [63]. The presence of angular mineral grains among the main mineral suite is very frequent at the outer shelf, shelf break and upper continental slope (depths > 120 m). The presence of such particles could result from the selective transport of river borne terrigenous particles into deeper areas of the continental shelf/upper slope domains without a long residence in higher energy environments (such as the inner shelf or littoral zones). Thus, the sedimentary history of these angular mineral grains may coincide with the one deduced from the quartz immature grains found at the shelf break [63]. It is also possible to consider the hypothesis that some angular heavy minerals were sourced and transported into the continental shelf deeper areas/upper slope during periods of lower sea levels. During these periods, they would have been directly transported into these areas without a long exposure to the intense dynamic processes that characterize shallow water environments (inner shelf and littoral zones). This is likely to have happened during the Last Glacial Maximum period (18,000 BP) when the environmental conditions allowed the transportation of large numbers of terrigenous particles by rivers into the continental slope [71,72]. This interpretation could explain the morphological similarities between the mineral grains identified in the Porto, Aveiro, and Nazaré areas and the ones observed either on the inner continental shelf or in the Northern Portuguese river sediments [12,33,34]. As such, it can be said that the main heavy mineral assemblage (amphibole, biotite, andalusite, tourmaline, garnet, staurolite, zircon, and apatite) includes the presence of "first-cycle" specimens recognized by their angular to very angular grain surface textures. Additionally, this heavy mineral assemblage includes the presence of "multi-cycle" mineral grains identified by their rounded to very rounded surface textures (Figure 19). All these mineral grains have a distal source either represented by the felsic igneous and metamorphic rocks of the NW Iberian Massif (angular ones) or by the reworked relict sediments from the continental shelf (rounded ones). The influence of the local source is recognized by the presence of pyroxene (diopside-hefenbergite, augite, enstatite-ferrosilite), amphibole (pargasite), and olivine (forsterite), mineral grains which always appear with angular surface textures and, in some sporadic cases, with euhedral forms. They can also be considered as "first-cycle" mineral grains although delivered from a local source (Figure 19, mineral grains #17–#22).

5.5. Heavy Mineral Source Synthesis

Figure 23 represents the synthesis of the main mineralogical sources. This synthesis considers the influence of distal and local sources. The distal ones are responsible for supplying the most representative mineralogical species: amphibole, andalusite, tourmaline, biotite, garnet, staurolite, zircon, and apatite. These minerals exhibit angular ("first-cycle" mineral grains) or rounded shapes ("multi-cycle" mineral grains). Local sources, in turn, are responsible for supplying pyroxene (diopside-hedenbergite, augite, enstatite-ferrosilite), amphibole (pargasite), and olivine (forsterite) mineral grains. These minerals have always angular or, in more sporadic situations, euhedral forms ("first-cycle" mineral grains).
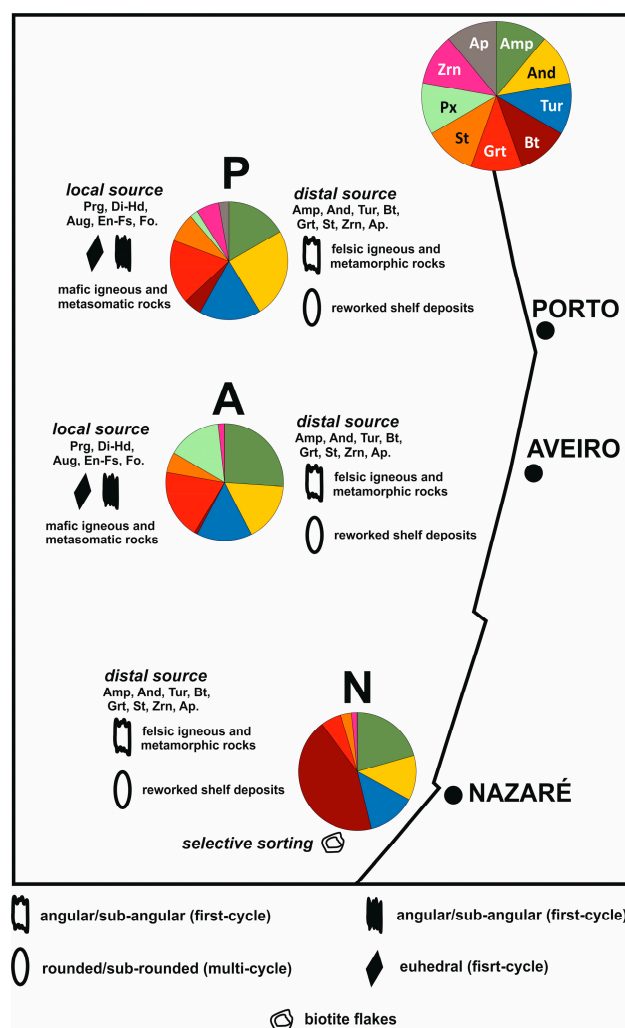
Figure 23. Heavy mineral source synthesis considering the 78 collected samples from the Porto (P), Aveiro (A), and Nazaré (N) areas. Distal and local sources are responsible for two different kinds of supplied minerals. The distal sources are responsible for the presence of angular mineral grains with fresh surface textures, considered as "first-cycle" detrital particles. They are also responsible for the presence of rounded mineral grains that are considered as "multicycle" detrital particles. The felsic igneous and metamorphic rocks of the Iberian Massif and derived terrigenous sediments are the main source of the angular mineral grains and the reworked relict-sedimentary deposits of the continental shelf are the main source of the rounded mineral grains. The mineral grains compatible with these distal sources are: amphiboles (Amp), andalusite (And), tourmaline (Tur), biotite (Bt), garnet (Grt), staurolite (St), zircon (Zrn), and apatite (Ap). Basic igneous rocks and thermal metamorphized dolomitic limestones are the most likely sources of the mineral assemblage derived from the local sources. This mineral assemblage is composed of diopside-hedenbergite (Dp-Hd), augite (Aug), enstatite-ferrosilite (En-Fs), pargasite (Prg) and forsterite (Fo). In the Nazaré area, a high concentration in biotite is observed due to the physical grain sorting of the lamellar mineral grains of this specimen.

6. Conclusions

This study identified the fundamental processes that control the presence of heavy minerals in three distinct areas of the Western Portuguese continental margin: the Porto, Aveiro, and Nazaré canyon head areas. In a broad view, the main heavy mineral assemblage identified in each area is composed by amphibole, andalusite, tourmaline, biotite, garnet, staurolite, pyroxene, zircon, and apatite. However, each studied area has a specific mineral signature that is controlled mainly by the source influence and, in a secondary plan, by the physical mineral grain sorting. In the Porto area,

the high frequency of andalusite, amphibole, tourmaline and garnet marked the specificity of the heavy mineral signature. In the Aveiro area, the high frequency of amphibole and pyroxene stood out as a distinctive mineral assemblage. In the Nazaré area, the extreme high frequency of biotite showed the peculiarity of the heavy mineral suite. Together, these results point to the influence of distal sources (erosion of the Iberian Massif rocks) as a fundamental factor in controlling heavy mineral variability. The specific influence of some geological formations of the Iberian Massif can be recognized by the chemical composition of garnets and amphiboles identified all over the Northern Portuguese continental shelf and in the Porto canyon head area. Granites, metamorphic rocks of amphibolitic and granulitic facies, are the most important sources for the identified garnets. However, in the Porto area the source of garnets seems to be limited to the referred metamorphic rocks. Most of the chemical composition of amphiboles is compatible with magnesio-hornblende and for that reason they were sourced from several types of metamorphic rocks (amphibolite and schist). The high frequency of biotite detected at the Nazaré area reflects the peculiar oceanographic setting of this canyon head area and, simultaneously, illustrates what is known as "hydraulic sorting", where the lamellar fine sand-sized biotite particles are concentrated in finer sediments that are preferentially transported together as a suspended load. The peculiar presence of pyroxene and olivine mineral grains at the Porto and Aveiro areas indicates the influence of specific local sources corresponding to basic igneous rocks and dolomitic limestone rocks affected by thermal metamorphism. This hypothesis is supported by the seismic data collected near the Porto canyon head area and by the chemical composition of several mineral grains of the referred species, confirming the presence of diospside-hedenbergite, augite, enstatite-ferrosilite and forsterite. Additionally, the presence of pargasite also supports the existence of an igneous basic source.

Conflicts of Interest: The author declares no conflict of interest.

References

1. Hazen, R.M. Evolution of minerals. *Sci. Am.* **2010**, *302*, 58–65. [CrossRef] [PubMed]
2. Morton, A.C.; Hallsworth, C.R. Processes controlling the composition of heavy minerals assemblages in sandstones. *Sediment. Geol.* **1999**, *124*, 3–29. [CrossRef]
3. Mange-Rajetzky, M.A. Sediment dispersal from source to shelf on an active continental margin, S. Turkey. *Mar. Geol.* **1983**, *52*, 1–26. [CrossRef]
4. Clemens, K.E.; Komar, P.D. Tracers of Sand Movement on the Oregon Coast. In *Coastal Engineering*; M.ASCE: Reston, VA, USA, 1998; pp. 1338–1351.
5. Komar, P.D. The Entrainment, Transport and Sorting of Heavy Minerals by Waves and Currents. In *Developments in Sedimentology*, 1st ed.; Mange, M.A., Wright, D.T., Eds.; Elsevier: Amsterdam, The Netherlands, 2007; Volume 58, pp. 3–48.
6. Garzanti, E.; Vermeesch, P.; Andò, S.; Lustrino, M.; Padoan, M.; Vezzoli, G. Ultra-long distance littoral transport of Orange sand and provenance of the Skeleton Coast Erg (Namibia). *Mar. Geol.* **2014**, *357*, 25–36. [CrossRef]

7.   Emery, K.O. Continental shelf sediments of southern California. *Geol. Soc. Am. Bull.* **1952**, *63*, 1105–1108. [CrossRef]

8.   Swift, D.J.; Stanley, D.J.; Curray, J.R. Relict sediments on continental shelves: A reconsideration. *J. Geol.* **1971**, *79*, 322–346. [CrossRef]

9.   Cascalho, J.P. Minerais Pesados: Aplicação ao Estudo da Dinâmica Sedimentar da Plataforma Continental Setentrional Portuguesa. Master's Thesis, Lisbon University, Lisbon, Portugal, 1993; 140p.

10.   Cascalho, J. Mineralogia dos Sedimentos Arenosos da Margem Continental Setentrional Portuguesa. Ph.D. Thesis, Lisbon University, Lisbon, Portugal, 2000; 400p.

11.   Ribeiro, M. *Dinâmica Sedimentar da Cabeceira do Canhão Submarino da Nazaré*; Scientific Report; Lisbon University: Lisbon, Portugal, 2008; 77p.

12.   Cascalho, J.; Fradique, C. The Sources and Hydraulic Sorting of Heavy Minerals on the Northern Portuguese Continental Margin. In *Developments in Sedimentology*, 1st ed.; Mange, M.A., Wright, D.T., Eds.; Elsevier: Amsterdam, The Netherlands, 2007; Volume 58, pp. 75–110.

13.   Rodrigues, A. Tectono-Estartigrafia da Plataforma Continental Setentrional Portuguesa. Ph.D. Thesis, Lisbon University, Lisbon, Portugal, 2001.

14.   Duarte, J.F. Distribuição Espacial dos Sedimentos do Canhão da Nazaré e Plataforma Adjacente. In Proceedings of the Assembleia Luso-Espanhola de Geodesia e Geofísica, Valência, Spain, 4–8 February 2002; Garcia, F.G., Valero, J.L.B., Eds.; Volume Tomo III, pp. 1162–1666.

15.   De Stigter, H.C.; Boer, W.; de Jesus Mendes, P.A.; Jesus, C.C.; Thomsen, L.; van den Bergh, G.D.; van Weering, T.C. Recent sediment transport and deposition in the Nazaré Canyon, Portuguese continental margin. *Mar. Geol.* **2007**, *246*, 144–164. [CrossRef]

16.   Oliveira, A.; Santos, A.I.; Rodrigues, A.; Vitorino, J. Sedimentary particle distribution and dynamics on the Nazaré canyon system and adjacent shelf (Portugal). *Mar. Geol.* **2007**, *246*, 105–122. [CrossRef]

17.   Guerreiro, C.; Oliveira, A.; Rodrigues, A. Shelf-break canyons versus "Gouf" canyons: A comparative study based on the silt-clay mineralogy of bottom sediments from Oporto, Aveiro and Nazaré submarine canyons (NW off Portugal). *J. Coast. Res.* **2009**, *SI 56*, 722–726.

18.   Vanney, J.R.; Mougenot, D. La Plate-Forme Continentale du Portugal et les Provinces Adjacentes: Analyse Geomorphologique. *Mem. Serv. Geo. Portugal.* **1981**, *28*, 86.

19.   Magalhães, F. A Cobertura Sedimentar da Plataforma Continental Portuguesa. Distribuição Espacial. Contrastes Temporais. Potencialidades Económicas. Ph.D. Thesis, Lisbon University, Lisbon, Portugal, 1999.

20.   Pombo, J. Sedimentos Superficiais da Plataforma Continental Portuguesa Entre o Cabo Mondego e S. Martinho do Porto. Master's Thesis, Coimbra University, Coimbra, Portugal, 2004.

21.   Rodríguez Fernández, L.R.; López Olmedo, F.; Oliveira, J.T.; Medialdea, T.; Terrinha, P.; Matas, J.; Martín-Serrano, A.; Martín Parra, L.M.; Rubio, F.; Marín, C.; et al. *Mapa Geológico de la Península Ibérica, Baleares y Canarias a escala 1: 1.000. 000*; IGME: Madrid, Spain, 2015.

22.   Carvalho, G. *Les Minéraux Lourds et la Paléogéographie des Dépôts Pliocènes du Portugal (Région Entre Vouga et Mondego)*; Museu e Laboratório Mineralógico e Geológico Centro de Estudos Geológicos: Coimbra, Portugal, 1954; Volume 37, pp. 61–64. Available online: http://hdl.handle.net/10316.2/38022 (accessed on 28 May 2019).

23.   Teixeira, C. *Notícia explicativa da folha 1-A (Valença) da Carta Geológica de Portugal na escala 1:50 000*; Serviços Geológicos de Portugal: Lisboa, Portugal, 1956; 16p.

24.   Costa, C.J.; Teixeira, C. *Notícia explicativa da folha 5-A (Viana do Castelo) da Carta Geológica de Portugal na escala 1:50 000*; Serviços Geológicos de Portugal: Lisboa, Portugal, 1957; 38p.

25.   Teixeira, C.; Assunção, C.T. *Notícia explicativa da folha 1-C (Caminha) da Carta Geológica de Portugal na escala 1:50 000*; Serviços Geológicos de Portugal: Lisboa, Portugal, 1961; 41p.

26.   Teixeira, C.; Medeiros, A.C.; Assunção, C.T. *Notícia explicativa da folha 9-A (Póvoa de Varzim) da Carta Geológica de Portugal na escala 1:50 000*; Serviços Geológicos de Portugal: Lisboa, Portugal, 1965; 50p.

27.   Teixeira, C.; Medeiros, A.C.; Alves, C.A.M.; Moreira, M.M. *Notícia explicativa da folha 5-C (Barcelos) da Carta Geológica de Portugal na escala 1:50 000*; Serviços Geológicos de Portugal: Lisboa, Portugal, 1969; 49p.

28.   Teixeira, C.; Medeiros, A.C.; Coelho, A.P. *Notícia explicativa da folha 5-A (Viana do Castelo) da Carta Geológica de Portugal na escala 1:50 000*; Serviços Geológicos de Portugal: Lisboa, Portugal, 1972; 43p.

29.   Ribeiro, A.; Antunes, M.T.; Ferreira, M.P.; Rocha, R.B.; Soares, A.F.; Zbyszewski, G.; Almeida, F.M.; Carvalho, D.; Monteiro, J.H. *Introduction à la Géologie Générale du Portugal*; Serviços Geológicos de Portugal: Lisboa, Portugal, 1979.

30. Noronha, F.; Leterrier, J. *Complexo Metamórfico da Foz do Douro. Geoquímica e Geocronologia. Resultados Preliminares. Mem. n. 4*; Museu e Laboratório Mineralógico e Geológico da Faculdade de Ciências da Universidade do Porto: Porto, Portugal, 1995; pp. 769–774.

31. Dinis, P.A.; Soares, A.F. Stable and ultrastable heavy minerals of alluvial to nearshore marine sediments from Central Portugal: Facies related trends. *Sediment. Geol.* **2007**, *201*, 1–20. [CrossRef]

32. Fradique, C.; Cascalho, J. Sedimentary processes in Douro Estuary (Portugal). A heavy mineral study. *Thalassas* **2004**, *20*, 61–68.

33. Fradique, C.; Cascalho, J.; Drago, T.; Rocha, F.; Silveira, T. The meaning of heavy minerals in the recent sedimentary record of the Douro estuary (Portugal). *J. Coast. Res.* **2006**, *SI 39*, 165–169.

34. Fradique, C.; Cascalho, J.; Drago, T. Translucent heavy minerals from the Minho Estuary sedimentary record. In Proceedings of the Costal Hope Conference, Lisbon, Portugal, 24–29 July 2005; Freitas, M.D., Drago, T., Eds.; Faculdade de Ciências da Universidade de Lisboa: Lisboa, Portugal, 2005; pp. 62–63.

35. McManus, J. Grain size determination and interpretation. In *Techniques in Sedimentology*, 1st ed.; Tucker, M., Ed.; Blackell Science: Oxford, UK, 1988; Volume 3, pp. 63–85. ISBN 0-632-01361-3.

36. Galehouse, J.S. Counting grain mounts; number percentage vs. number frequency. *J. Sediment. Res.* **1969**, *39*, 812–815. [CrossRef]

37. Davis, J.C. *Statistics and Data Analysis in Geology*; John Wiley & Sons: New York, NY, USA, 1986; 646p.

38. Morton, A.C. A new approach to provenance studies: Electron microprobe analysis of detrital garnets from Middle Jurassic sandstones of the northern North Sea. *Sedimentology* **1985**, *32*, 553–566. [CrossRef]

39. Haughton, P.D.W.; Farrow, C.M. Compositional variation in Lower Old Red Sandstone detrital garnets from the Midland valley of Scotland and the Anglo-Welsh Basin. *Geol. Mag.* **1989**, *126*, 373–396. [CrossRef]

40. Morton, A.; Hallsworth, C.; Chalton, B. Garnet compositions in Scottish and Norwegian basement terrains: A framework for interpretation of North Sea sandstone provenance. *Mar. Pet. Geol.* **2004**, *21*, 393–410. [CrossRef]

41. Mange, M.A.; Morton, A.C. Geochemistry of heavy minerals. In *Developments in Sedimentology*, 1st ed.; Mange, M.A., Wright, D.T., Eds.; Elsevier: Amsterdam, The Netherlands, 2007; Volume 58, pp. 345–391.

42. Suggate, S.M.; Hall, R. Using detrital garnet compositions to determine provenance: A new compositional database and procedure. *Geol. Soc. Lond. Spec. Publ.* **2014**, *386*, 373–393. [CrossRef]

43. Locock, A.J. An Excel spreadsheet to recast analyses of garnet into end-member components, and a synopsis of the crystal chemistry of natural silicate garnets. *Comput. Geosci.* **2008**, *34*, 1769–1780. [CrossRef]

44. Locock, A.J. An Excel spreadsheet to classify chemical analyses of amphiboles following the IMA 2012 recommendations. *Comput. Geosci.* **2014**, *62*, 1–11. [CrossRef]

45. Hawthorne, F.C.; Oberti, R.; Harlow, G.E.; Maresch, W.V.; Martin, R.F.; Schumacher, J.C.; Welch, M.D. Nomenclature of the amphibole supergroup. *Am. Mineral.* **2012**, *97*, 2031–2048. [CrossRef]

46. Leake, B.E.; Woolley, A.R.; Arps, C.E.; Birch, W.D.; Gilbert, M.C.; Grice, J.D.; Hawthorne, F.C.; Kato, A.; Kisch, H.J.; Krivovichev, V.G.; et al. Nomenclature of amphiboles; report of the Subcommittee on Amphiboles of the International Mineralogical Association Commission on new minerals and mineral names. *Miner. Mag.* **1997**, *61*, 295–310. [CrossRef]

47. GabbroSoft. 2011. Available online: http://www.gabbrosoft.org/ (accessed on 29 May 2019).

48. Morimoto, N. Nomenclature of pyroxenes. *Mineral. Petrol.* **1988**, *39*, 55–76. [CrossRef]

49. Mange, M.A.; Maurer, H. *Heavy Minerals in Colour*, 1st ed.; Chapman: California, CA, USA, 1992; 147p.

50. Andò, S.; Garzanti, E.; Padoan, M.; Limonta, M. Corrosion of heavy minerals during weathering and diagenesis: A catalog for optical analysis. *Sediment. Geol.* **2012**, *280*, 165–178. [CrossRef]

51. Sousa, M.B. Skarns e rochas calco-silicatadas do Complexo xisto-grauváquico do Douro (NE de Portugal)—seu enquadramento litoestratigráfico. *Com. Serv. Geol. Port.* **1981**, *67*, 169–172.

52. Coelho, J.M.D. Os" Skarns" Cálcicos, Pós-Magmáticos, Mineralizados em Scheelite do Distrito Mineiro de Covas, VN de Cerveira, (Norte de Portugal). Ph.D. Thesis, Porto University, Porto, Portugal, 1990; 345p. Available online: http://hdl.handle.net/10216/10227 (accessed on 20 May 2019).

53. Gomes, G.L. Spatial simulation of the W-Sn ore Grades of São Pedro das Águias Skarn Mineral Deposit (Tabuaço, Northern Portugal). Ph.D. Thesis, Porto University, Porto, Portugal, 2016; 102p. Available online: https://run.unl.pt/handle/10362/18446 (accessed on 20 May 2019).

54. Niida, K. Kaersutite, Ti-pargasite, and pargasite from gabbroic rock of the Horoman ultramafic massif, Japan. *J. Jpn. Assoc. Mineral. Petrol. Econ. Geol.* **1977**, *72*, 152–161. [CrossRef]

55. Deer, W.A.; Howie, R.A.; Zussman, J. *An Introduction to the Rock-Forming Minerals*, 2nd ed.; Prentice Hall: Harlow, UK, 1992; 558p.

56. Cascalho, J.; Carvalho, A.M.G. Proveniência dos minerais pesados da plataforma continental portuguesa a norte do paralelo de Espinho. *Gaia* **1993**, *6*, 10–25.

57. Rodrigues, A.; Cascalho, J.; Ribeiro, A.; Dias, J.M.A. *Evidências de actividade vulcânica nas cabeceiras do canhão submarino do Porto. Memórias n. 4*; Museu e Laboratório Mineralógico e Geológico da Faculdade de Ciências da Universidade do Porto: Porto, Portugal, 1995; pp. 305–309.

58. Meinert, L.D. Skarns and skarn deposits. *Geol. Can.* **1992**, *19*, 145–162.

59. Mazurov, M.P.; Grishina, S.N.; Istomin, V.E.; Titov, A.T. Metasomatism and ore formation at contacts of dolerite with saliferous rocks in the sedimentary cover of the southern Siberian platform. *Geol. Ore Dep.* **2007**, *49*, 271–284. [CrossRef]

60. Mazurov, M.P.; Grishina, S.N.; Titov, A.T.; Shikhova, A.V. Evolution of Ore-Forming Metasomatic Processes at Large Skarn Iron Deposits Related to the Traps of the Siberian Platform. *Petrology* **2018**, *26*, 265–279. [CrossRef]

61. Gallien, F.; Abart, R.; Wyhlidal, S. Contact metamorphism and selective metasomatism of the layered Bellerophon Formation in the eastern Monzoni contact aureole, northern Italy. *Mineral. Petrol.* **2007**, *91*, 25–53. [CrossRef]

62. Garzanti, E.; Andò, S.; Vezzoli, G. Settling equivalence of detrital minerals and grain-size dependence of sediment composition. *Earth Plane. Sci. Lett.* **2008**, *273*, 138–151. [CrossRef]

63. Dias, J.M.A.; Nittrouer, C.A. Continental shelf sediments of northern Portugal. *Cont. Shelf Res.* **1984**, *3*, 147–165. [CrossRef]

64. Quaresma, L.S.; Vitorino, J.; Oliveira, A.; da Silva, J. Evidence of sediment resuspension by nonlinear internal waves on the western Portuguese mid-shelf. *Mar. Geol.* **2007**, *246*, 123–143. [CrossRef]

65. Neiheisel, J. Source and distribution of sediments at Brunswick Harbour and vicinity, Georgia. U.S. Army Coastal Engineering. *Cent. Tech. Memo.* **1965**, *12*, 21.

66. Pomerancblum, M. The distribution of heavy minerals and their hydraulic equivalence in sediments of the Mediterranean continental slope of Israel. *J. Sediment. Res.* **1966**, *36*, 162–174. [CrossRef]

67. Doyle, L.J.; Clearly, W.J.; Pilkey, O.H. Mica: Its use in determining shelf depositional regimes. *Mar. Geol.* **1968**, *6*, 381–389. [CrossRef]

68. Doyle, L.J.; Carder, K.L.; Steward, R.G. The hydraulic equivalence of mica. *J. Sediment. Res.* **1983**, *53*, 643–648. [CrossRef]

69. Adegoke, O.S.; Stanley, D.J. Mica and shell as indicators of energy level and depositional regime on the Nigerian shelf. *Mar. Geol.* **1972**, *13*, M61–M66. [CrossRef]

70. Kuenen, P.H. Experimental abrasion: 6. surf action. *Sedimentology* **1964**, *3*, 29–43. [CrossRef]

71. Rodrigues, A.; Magalhães, F.; Dias, J.A. Evolution of the North Portuguese coast in the last 18,000 years. *Quat. Int.* **1991**, *9*, 67–74. [CrossRef]

72. Dias, J.M.A.; Boski, T.; Rodrigues, A.; Magalhães, F. Coast line evolution in Portugal since the Last Glacial Maximum until present—A synthesis. *Mar. Geol.* **2000**, *170*, 177–186. [CrossRef]